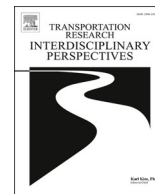


Contents lists available at [ScienceDirect](https://www.sciencedirect.com)

# Transportation Research Interdisciplinary Perspectives

journal homepage: [www.sciencedirect.com/journal/transportation-research-interdisciplinary-perspectives](https://www.sciencedirect.com/journal/transportation-research-interdisciplinary-perspectives)



## A predictive cellular automata framework with SSA-LSTM and ACC for safe and efficient autonomous driving

Tao Yufei<sup>a</sup>, Husam A. Neamah<sup>a,b,\*</sup> 

<sup>a</sup> Department of Electrical Engineering and Mechatronics, Faculty of Engineering, University of Debrecen, Ótemető Utca 2-4, 4028 Debrecen, Hungary

<sup>b</sup> Technical Engineering College, Al-Ayen University, Thi-Qar 64001, Iraq

### ARTICLE INFO

#### Keywords:

Intelligent Transportation System  
Stability Analysis  
Machine Learning Algorithms  
Traffic Safety  
Long Short-Term Memory  
Cellular Automata (CA) Model

### ABSTRACT

This research proposes a multi-model combinatorial congestion mitigation approach to solve the traffic safety problem and speed optimisation problem of autonomous vehicles. The proposed model framework consists of three parts: a road modelling module based on meta cellular automata, a traffic flow speed prediction module consisting of an optimised long and short-term memory algorithm using a sparrow search algorithm, and a following distance prediction module that determines the optimal safe following distance using an adaptive cruise control algorithm. In the simulation, this intelligent traffic model for autonomous cars can be applied to various complex traffic scenarios based on the design of real traffic intersections, which improves traffic efficiency while reducing the collision risk of autonomous vehicles. After setting up a control group experiment to verify, compared with the traditional optimisation algorithm, the algorithm model designed in this study significantly improves the prediction ability of the autonomous vehicle when subjected to traffic pressure. In the one-hour simulation experiment process, the vehicle's average speed was increased by at least 3.89%. At the same time, the judgement of the safety distance of the following car was also made ahead of time, which made the vehicle drive more smoothly. When dealing with traffic congestion caused by accidents on the road, the average queue length of vehicles was reduced by 92.86%, and the maximum queue length was decreased by 78.57%.

### 1. Introduction

In autonomous driving system, predicting traffic flow speed and following distance is crucial. Most existing studies fail to consider the impact of the traffic environment (i.e., traffic levels and vehicle types) on traffic flow speed. As a result, these models cannot effectively adapt to real-world traffic conditions. This study aims to address this issue by utilizing Cellular Automata (CA) modelling to simulate roads and traffic flow. Additionally, it predicts the safe range of traffic flow speed and following distance to maximize traffic efficiency at congested intersections while ensuring safety. Traditional traffic control methods face multiple challenges against the gradual development of global transport systems towards intelligence and synergy. Fixed-cycle signals, follow-up control with lagging response, and distributed traffic scheduling mean that lack of learning capability often makes it challenging to maintain stable operation when dealing with urban road networks with dramatic fluctuations in traffic density and frequent complex disturbances (Moreno-Malo et al., 2024). In order to solve these problems, a

large number of researches in recent years have focused on combining sensory data, prediction models and real-time control strategies to build intelligent traffic control systems with active response capability (Liu, 2024). This trend is based on the core logic of “prediction first + dynamic adjustment”, which allows the traffic system to identify trends, predict risk, and optimise behaviour (Tan et al., 2025).

Moreover, with this trend, the advantages of autonomous driving are gradually being noticed. According to Montanaro et al. (2019), connected autonomous cars are considered an effective means of alleviating the problems of traffic congestion, road safety, inefficient fuel consumption and pollutant emissions currently facing the road traffic system (Montanaro et al., 2019). Mimicking human behavioural logic and designing automated driving systems is the future direction of intelligent transport development (Almusawi et al., 2022; Neamah and Butdee, 2024b; Neamah and Mayorga Mayorga, 2024; Xu et al., 2024b).

In general, mainstream intelligent traffic control methods can be divided into three categories: rule-based control methods, optimisation control methods and data-driven control methods. Rule-based control

\* Corresponding author at: Otemeto Utca 4-5, 4028 Debrecen, Hungary.

E-mail address: [husam@eng.unideb.hu](mailto:husam@eng.unideb.hu) (H.A. Neamah).

<https://doi.org/10.1016/j.trip.2025.101828>

Received 9 June 2025; Received in revised form 25 December 2025; Accepted 26 December 2025

Available online 9 March 2026

2590-1982/© 2025 The Author(s). Published by Elsevier Ltd. This is an open access article under the CC BY license (<http://creativecommons.org/licenses/by/4.0/>).

strategies rely on fixed logic rules for response (Neamah et al., 2024c; Tsuchimochi et al., 2023).

There are several issues automated driving needs to deal with when facing traffic road conditions (Masuk et al., 2022; Yan et al., 2024). De Gelder et al. (2022) argue that developing new methods for assessing the performance of autonomous vehicles is crucial for deploying autonomous technology due to the complexity of the field in which they operate (De Gelder et al., 2022). Given the complexity of the realities modelled by real scenarios, defining a structure to capture them is challenging. An inward-looking definition can provide a set of characteristics considered necessary and sufficient for the scenarios, thus ensuring that the constructed scenarios are complete and comparable (Katona et al., 2024; Nilsson et al., 2017; Nyangaresi et al., 2024).

Beyond that, researchers have raised many more concerns. Czarniecki (2018a) presented a theoretical model that can be used to design autonomous driving systems, providing a solid foundation for the concept of autonomous driving (Czarniecki, 2018b). This research considers factors such as pedestrians, unexpected obstacles, and environmental changes and provides ideas for a multifaceted approach to safeguarding the safety design of autonomous driving systems (Hu et al., 2024); (Bryant and Huson, 2023). The theories in this study can help more researchers better simulate and master the complex traffic environment in reality. A study by Di Lillo et al. (2024) assessed the safety performance of autonomous cars in different traffic environments by analysing real-world driving data (Di Lillo et al., 2024; Neamah et al., 2024b; Neamah and Butdee, 2024a).

With the advent of the smart era, driverless vehicles have gradually taken over a larger and larger part of the transport market (Elrofai et al., 2016). A lot of people will choose driverless vehicles to travel, or use driverless technology to improve their lives (Nath et al., 2020). However, driverless technology is still in the development stage, and both its judgement and safety factor need to be strengthened (Amir Siddique et al., 2021). There are a large number of studies on intelligent transport systems, but the judgement of driverless vehicles in complex road conditions has not always been satisfactory, often leading to dangerous situations, which will deepen people's concern about the future of intelligent transport development (Baqa et al., 2021). Abdel-Aty and Ding (2024) study the differences in accident rates between autonomous and human-driven vehicles using a large amount of driving data and information from simulation experiments stored in a database (Abdel-Aty and Ding, 2024); (Gao et al., 2023).

In such a case, a more rigorous parameter design is necessary to facilitate the subsequent putting of the research into practical applications (Abdessalem et al., 2018b). Nevertheless, times are changing rapidly, and another renewed challenge has been faced on today's traffic roads (Ranpura et al., 2025). However, using vehicles to simulate real traffic conditions may still be a good option (Jin et al., 2024). The practical consideration of vehicle parameters in the design of the experimental scenarios gives the experimental results more possibilities to be applied flexibly in reality (Chen, 2024).

After much research and validation, autonomous driving technology already possesses judgement beyond human drivers (Katz-Samuels et al., 2021). Chen et al. (2018) proposed a new real-time decision-making framework to deal with complex traffic environments and improve autonomous vehicles' decision-making efficiency and safety under dynamic conditions (Chen et al., 2018). This study significantly improves the adaptability and reliability of autonomous vehicles in complex traffic scenarios (Chen et al., 2018); (Wang and Li, 2020). Wang et al. (2021) proposed a single-step dynamic game lane-changing decision based on incomplete information and Bézier curve-based path planning to coordinate the lane-changing performance of vehicles in terms of safety payoffs, speed payoffs and comfort payoffs (Wang et al., 2021). The results of the three lane-changing scenarios designed in the hardware loop experiments show that the vehicle controlled by the proposed method outperforms the human driver in terms of safety, dynamics, and passenger comfort in both discretionary and forced lane-

changing scenarios (Wang et al., 2021); (Luo et al., 2021).

Of the many studies, it is worth noting that Zhang et al. considered the average speed of downstream vehicles, so they hoped to know the traffic condition of the downstream road through prediction (Zhang et al., 2024). This is similar to the design concept in this experiment. Their proposed car-following model was shown during the experiments to help stabilise traffic safety by suppressing and minimising the formation of traffic oscillations as much as possible through the modelling algorithm, which can help vehicles to form up more quickly. The methodology provides a good fit for realistic data and helps car drivers understand the traffic conditions downstream of the road in advance (Zhang et al., 2024); (Abdessalem et al., 2018a).

In summary, the research of intelligent traffic control methods gradually shifts from rule response to learning prediction, and the control strategy also shifts from state feedback to trend guidance (Zhang et al., 2018). In this context, constructing a unified system capable of integrating traffic flow modelling, in-depth prediction, and real-time control is an inevitable trend of technological evolution and a practical impetus for the development of autonomous driving and intelligent urban transportation (Kóvári et al., 2021).

Traffic intersections located near residential areas are often characterized by high upstream traffic volumes, which consequently lead to reduced downstream traffic safety. This issue becomes particularly critical during peak traffic periods, as ensuring that autonomous vehicles maintain a stable speed and a safe following distance within the traffic flow remains a significant challenge.

This research focuses on speed prediction and following behaviour regulation methods in automatic driving micro-control scenarios, and constructs a traffic simulation and control system that combines meta-cellular automata modelling, intelligent prediction models and behavioural controllers. The goal of the research is to improve the rhythmic consistency, safety margin and system stability of traffic operation.

In this study, a three-lane intersection was modelled as the upstream intersection in the experimental environment, while an intersection extending from a residential area was set as the downstream intersection. This setup comprehensively considers both traffic efficiency and safety. Furthermore, the speed and following distance of autonomous vehicles were regulated. The results indicate that the LSTM-based traffic flow optimisation significantly enhances traffic efficiency, while the integration with the ACC algorithm ensures traffic safety. Moreover, CA-based modelling enables the system to handle unexpected road conditions, demonstrating the model's adaptability to various environments. The proposed model can be applied to diverse traffic scenarios to improve traffic efficiency, mitigate collision risks for autonomous vehicles, and enhance traffic management and autonomous driving safety.

## 2. Research methodology

With the rapid progress of Intelligent Transportation Systems (ITS), the value of data-driven predictive control methods based on data is becoming increasingly evident in the application of autonomous driving and cooperative sensing traffic management. In order to construct a longitudinal control system with response foresight and operational stability, the integration of traffic flow modelling theory, predictive algorithms and intelligent control mechanisms has become a key direction of current research.

### 2.1. Reference and application of traffic flow modelling theory

Traffic flow modelling is a fundamental part of ITS research, and its primary goal is to describe the behavioural patterns of traffic participants in time and space and build mathematical models or rule systems accordingly to support prediction, optimisation and control tasks (Schütt et al., 2023). The cellular automata (CA) model is usually applied to single or multi-lane traffic flow modelling and has a special performance in a part of the analysis application field when dealing with

complex intersections and unexpected events (Neamah et al., 2024a; Shafaei et al., 2018). For example, when dealing with road emergencies, the cellular automata (CA) can mark the locations of the emergencies on the road, which has a good scope of application in the field of road de-escalation (M. Zhang et al., 2016). The discrete nature of CA models allows them to show superior computational efficiency when dealing with large-scale complex traffic problems, but how to further apply their prediction accuracy remains one of the key topics in current research (Czarnecki, 2018a).

In the experiments, the meta cellular automata, in addition to simulating the experimental scenarios, can be combined with the ACC algorithm to allow autonomous vehicles to avoid obstacles in advance in conjunction with the prediction algorithm (Thorn et al., 2018). Eskandarian (2024), who also worked on the autonomous car topic, attempted to improve the driving function through algorithms that would allow it to do lane changing, merging, and automatic intersection navigation better on its own, as well as training in scenarios with possible collision scenarios to increase safety (Eskandarian, 2024). Similarly, Zhang et al. (2025) proposed a trajectory-planning method for intelligent vehicles' lane-changing problem. The method can vary flexibly according to road characteristics (Zhang et al., 2025); (He and Lv, 2023).

This study's primary reference for the meta cellular automata simulation approach comes from Li et al (Li et al., 2021). How roads are segmented into tuples and vehicles and other road parameters are modelled and integrated with experiments are similar approaches in many research designs (Xu et al., 2025).

## 2.2. Design of predictive algorithms and intelligent control mechanisms

The prediction algorithm applied in this study combines a sparrow search algorithm with a long and short-term memory algorithm (Ben Abdesslem et al., 2016), as shown in Fig. 1. The traditional rule-based control strategy usually adopts the closed-loop feedback mode of "speed difference-distance difference", which triggers braking or deceleration when the system senses that the distance between the vehicle and the vehicle in front decreases (Rong et al., 2020). This strategy is characterised by simple logic and low implementation cost. However, there is an obvious hysteresis problem: the system can only react passively based on the current state (Xu et al., 2024a). It cannot predict the upcoming speed change or distance reduction, which is prone to trigger the phenomenon of "chained deceleration" and the propagation of cadence

perturbation (Sarraf et al., 2020; Su and Zhang, 2024).

Many researchers have made their algorithm design. Ghodsi et al. (2021) proposed an efficient de-escalation mechanism tested using a state-of-the-art driving simulator based on real-world data, modelling scenarios and generating vehicle failure cases in a simulation (Ghodsi et al., 2021). Thus, it is possible to define metrics based on the complexity of avoiding accidents, rank scenarios, and minimise the probability of accidents (Ghodsi et al., 2021); (Huang and Lv, 2021). Ban et al. (2022) focused on improving neural active learning algorithms and optimising the data selection process through a new sampling strategy to improve the model's training efficiency and generalisation ability (Ban et al., 2022; Cabrejas-Egea et al., 2021).

In contrast, the SSA-LSTM control model has forward prediction capability and a dynamic parameter adjustment mechanism (Han et al., 2024). By integrating the SSA optimisation method to optimise the parameters of the LSTM network, the model can extract the vehicle speed evolution characteristics within the sliding time window and predict the speed trend in the next three steps. As a result, the controller can issue acceleration and deceleration commands in advance, realising "front-loading" and significantly reducing the risk of sudden tempo changes. This structural difference makes SSA-LSTM more suitable for dealing with complex, dynamic and uncertain traffic flow scenarios.

When sampling and evaluating real-world scenarios, it is essential to consider that traditional control models perform reasonably well on straight roads with simple structures, single-lane traffic, or low-density jetting conditions. However, their lag and local over-intervention problems are significantly exacerbated in unexpected situations such as multi-vehicle mixing, lane convergence and traffic accidents, which make it difficult to maintain the overall rhythm of the system. In contrast, the SSA-LSTM controller combines the dual advantages of model-driven and data-driven approaches, which can learn potential trends based on historical behavioural sequences and adapt to different types of vehicles, traffic densities, and complex traffic structures while ensuring prediction accuracy.

In summary, time series forecasting models are a key component of intelligent control systems for trend sensing and advanced decision-making (Cardoso et al., 2023). Among various modelling methods, LSTM has become one of the primary methods in traffic prediction due to its superior ability to express short-term trends and long-term dependencies. Combining predictive algorithms with other algorithms can also lead to better performance in experiments, such as using Adaptive

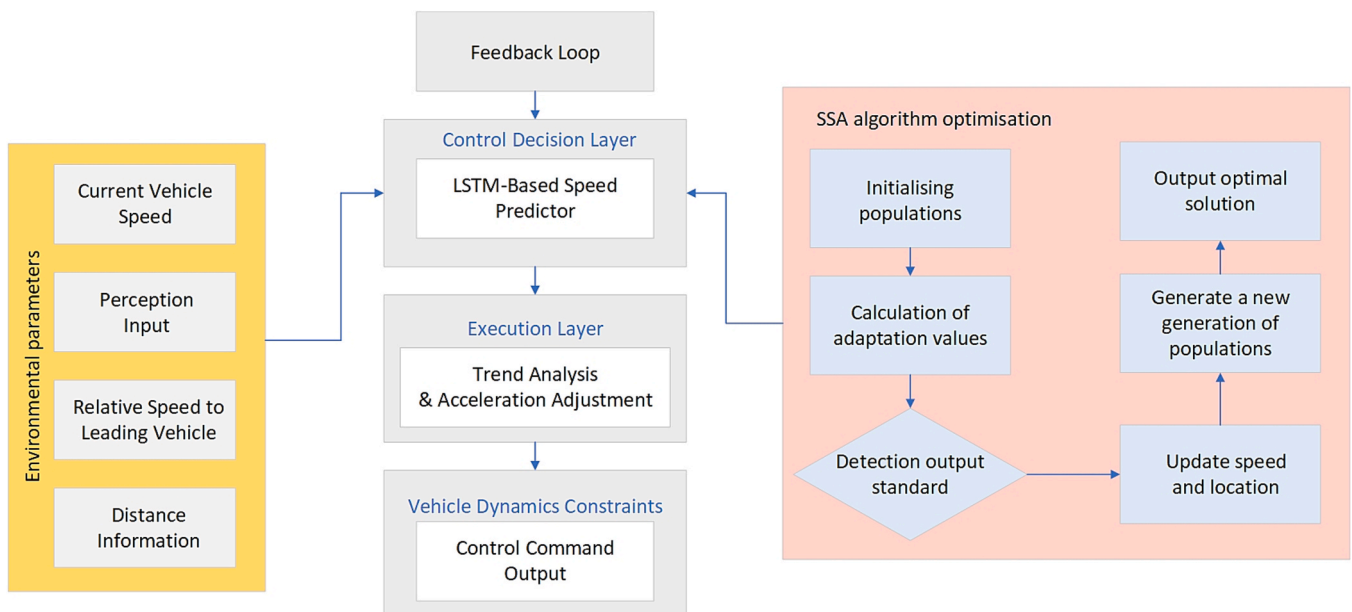


Fig. 1. Long and Short Term Memory Algorithm Optimised by Sparrow Search Algorithm.

Cruise Control (ACC) technology to control vehicle acceleration or deceleration (Francis et al., 2024).

Therefore, based on the current research content, it is clear that we should bravely face the challenges of intelligent traffic control technology, and there are many parts that deserve in-depth research in the exploration of the technology of driverless vehicles. Moreover, combining science and technology with life, so that science and technology can benefit human beings, is always the ultimate demand of scientific research. Accordingly, this study investigates the application of SSA-optimised long and short-term memory networks (SSA-LSTM) for traffic flow prediction, applying it to intelligent traffic simulation experiments, and exploring the coordination ability of intelligent traffic system combined with multi-faceted. This study not only combines the flexibility of *meta*-cellular automata modelling with the advantages of deep learning models in timing prediction, but also explores the feasibility and practical value of predictive behaviour-driven control in highly dynamic traffic environments, aiming to provide methodological support and experimental basis for constructing more efficient intelligent traffic control systems.

### 3. Cellular automata simulation

This study combines traffic modelling theory and deep learning techniques in the experimental design to establish a framework for an intelligent transport system that integrates modelling, prediction and control. The model shown in Fig. 2 is based on *meta*-cellular automata to simulate the real traffic environment. In complex, large-scale traffic networks, the traditional fixed-time signal control method can no longer meet the dynamically changing traffic demand, and according to the conclusions of recent existing research, the signal optimisation strategy based on machine learning has gradually become the mainstream research direction. A new framework needs to be proposed to improve

traffic flow prediction accuracy. The proposed model should be designed using better application functionality (Bharti et al., 2023).

Applying cellular automata (CA) in traffic road experiments is a valuable research option. As a discrete model, the cellular automaton (CA) shows significant advantages in simulating the dynamic behaviour of traffic flow. It can effectively capture the interactions between vehicles and the non-linear characteristics of traffic flow. It can better handle and analyse the road situation and present the road in the actual scenario as a modelling simulation, specifically in the experiment. At the same time, the CA model also has the function of being able to simulate different specifications of vehicles on the road, which can make the experimental simulation of the road situation more realistic, the traffic queue situation more in line with reality, and can therefore take into account the different scenarios caused by a variety of road conditions in the experiments, which is indispensable in the targeted research and an important reference (Xue et al., 2022).

The model implementation consists of several classes and function modules, including a road modelling module, a vehicle modelling module, a dispatch control module, and a simulation module. In this study, the discretisation rule is used to divide the road into tuples with a length of 2 m, and the vehicles are divided into various types (cars, trucks, buses), occupying 2, 3 and 5 consecutive tuples, respectively. Vehicle states include fields such as position, speed, vehicle type, index of the preceding vehicle, etc., and all states are stored in a global state table for access by the prediction model and controller module. In each time step, the system completes the whole process of “perception-prediction-control-execution”, the vehicle updates its state according to its control results, and the next cycle relies on the current state cache. Regarding CA model evolution rules, the system adopts the three-stage speed update mechanism, which includes maximum speed limit, forward collision avoidance determination, and behavioural trend correction module.

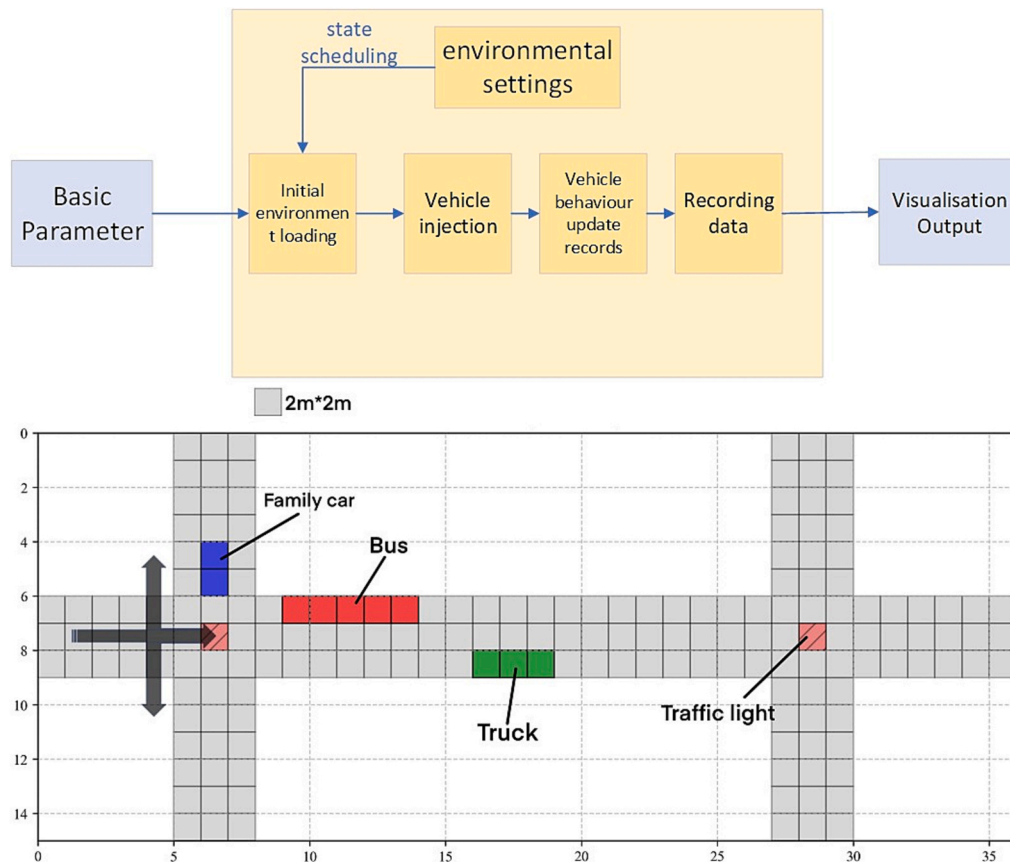


Fig. 2. Sparrow Search Algorithm Workflow and CA Modelling Diagram.

The scheduling control module consists of the Cellular-Automaton class as the core system scheduler, which calls the vehicle's behavioural functions at each time step to perform state updates, collision detection, and traffic state recording. The module also contains control mechanisms such as intersection conflict handling, yield logic, and lane change judgement to ensure that the simulated behaviour conforms to the real traffic rules. At the same time, the CA model also has the function of being able to simulate different specifications of vehicles on the road, which can make the experimental simulation of the road situation more realistic, the traffic queue situation more in line with reality, and can therefore take into account the different scenarios caused by a variety of road conditions in the experiments, which is indispensable in the targeted research and an important reference (Xue et al., 2022). In this system, each lane is divided into equal-length cell units (cells), and the state of each cell at each time step  $t$  depends on the state of itself and its neighbouring cells at time  $t-1$ . The system performs operations such as vehicle injection, position update, speed control, and steering decisions sequentially at each step, depending on the vehicle's state and the road structure. The speed update of the vehicle object is handled by the controller (e.g., ACC module), which outputs regulation decisions based on the current distance and the vehicle's state ahead. The road model Road manages the state of the meta cells of multiple lanes and records the distribution of each vehicle in the visual range to ensure that the system can monitor the traffic structure in real time.

Vehicle speed limit [cell/s]: The speed of each vehicle  $v_i(t)$  is satisfied.

$$v_i(t) \in [v_{\min}, v_{\max}], v_{\min} = 30 \text{ km/h}, v_{\max} = 60 \text{ km/h} \quad (1)$$

Safe distance determination: At any step  $t$ , the distance between vehicle  $i$  and the vehicle in front of  $i-1$ .

$$d_i(t) = x_{i-1}(t) - x_i(t) \quad (2)$$

where  $x_i(t)$  is the current position (in tuples) of vehicle  $i$ . The vehicle can accelerate only if  $d_i(t) > d_{\text{safe}}$ .

#### 4. Speed prediction via SSA-optimised LSTM model

##### 4.1. Research framework

In order to enhance the performance of traffic systems, intelligent optimisation algorithms have been gradually applied to the modelling of traffic flows. Sparrow Search Algorithm (SSA), as an emerging population intelligence optimisation method, imitates the behaviour of sparrow foraging with powerful global search capability and fast convergence speed. It has been applied with remarkable success in several fields. In recent years, SSA has achieved remarkable results in improving the performance of deep learning models, especially in parameter optimisation of LSTM networks. In optimising hyperparameters, SSA defines the search space, obtains traffic flow information, and initialises the sparrow population on the road simulated by the experiment. The important feature of the SSA optimisation algorithm is that the data in the population will observe each other's behavioural performance, which is precisely in line with the characteristics of the convoy waiting in line to pass the road; the rear vehicles will definitely judge their actions based on the behaviour of the vehicles in front of them, and this is also the reason why I chose the sparrow algorithm for the optimisation of the LSTM algorithm. In the process of iterative optimisation, the behaviour of the vehicle in front will drive the judgment of the vehicle at the back, and the speed space between each other will be split in detail in the algorithm. It allows the whole convoy to find the fastest speed, which is very suitable for the judgment of uncrewed vehicles, and it can provide the improvement of maximised optimisation for the judgment of the behaviours of the autonomous system. The SSA-optimised Long Short-Term Memory Network (LSTM) has demonstrated excellent adaptability and generalisation capabilities in the field of time

series prediction. The memory mechanism of LSTM can effectively handle the time series characteristics of traffic data, while the global search capability of SSA can further improve prediction accuracy. Combining these two is the best basis for intelligent behavioural judgment applicable to autonomous systems.

In terms of traffic flow optimisation, an approach that combines a Long Short-Term Memory Network (LSTM) with a Sparrow Search Algorithm (SSA) can improve the intelligence of signal control, reduce the waiting time for vehicles on the road, and enhance the capacity of intersections. This is especially applicable in congested roads with high traffic volume. It has been shown that using deep learning techniques to predict traffic flow states can more accurately optimise signal control, thereby significantly reducing the average waiting time of vehicles, which is exactly the point of optimising the traffic system. This improvement is further enhanced by combining more experimental approaches with deep learning models, which have been proven effective in recent traffic flow prediction tasks (Harrou et al., 2024). In complex, large-scale traffic networks, the traditional fixed-time signal control method can no longer meet the dynamically changing traffic demand, and according to the conclusions of recent existing research, the signal optimisation strategy based on machine learning has gradually become the mainstream research direction. A new framework needs to be proposed to improve traffic flow prediction accuracy. The proposed model should be designed using better application functionality (Bharti et al., 2023). By observing vehicle behaviour on the road, combined with the diverse data of road topography, congestion time, and vehicle types, learning the features in the experimental environment enables the analytical model to make further optimisation judgments to be applied to the decision-making of autonomous systems.

As shown in the Fig. 3, the SSA-LSTM algorithm, which forms the core of the entire system design, is a crucial component of this research. Extending from that core, the entire structure of the algorithm can be shown, with each module interacting with one another and data being passed between them to complete the process from input to prediction to output optimisation. As shown in the Fig. 3, the main modules of the system design are these three main functional layers: the first layer is the traffic environment modelling layer, which uses cellular automata (CA) to construct the basic microstructural model of the vehicle and the road system; the second layer is the prediction and analysis layer, which is based on the improved Long Short-Term Memory (LSTM) network model to make a time-series prediction of the future speed, and optimised by using the Sparrow Search Algorithm (SSA); The third layer is the control execution layer, which adopts the adaptive cruise control (ACC) strategy to dynamically adjust the following behaviour in the traffic flow, so that the autonomous vehicle can always maintain a safe distance and get effective safety control.

Based on the time series data generated by the CA model, this study employs an improved LSTM prediction model for speed prediction. Although the traditional LSTM model performs well in time series modelling, it still suffers from the shortcomings of slow decision-making and the inability to cope with multiple variations when dealing with traffic systems, a non-linear and highly noisy data source. For this reason, it was decided to use the Sparrow Search Algorithm (SSA) to fully optimise the key hyperparameters (e.g., hidden layer dimension, learning rate) of the LSTM model in order to improve the prediction accuracy and to enhance the model's adaptability under various traffic states significantly. The optimised LSTM model can not only accurately predict the speed trend of the vehicle in the future moments but also be used as an input to the ACC control module, which can provide a prospective reference basis for the vehicle following strategy.

At the distance control level, this study combines the adaptive cruise control (ACC) strategy to achieve dynamic adjustment of the safe distance between the target vehicle and the vehicle ahead. The ACC control model can calculate the optimal acceleration or deceleration value based on long-term, short-term memory (LSTM) prediction results and real-time vehicle distance. The control process can be visualised by

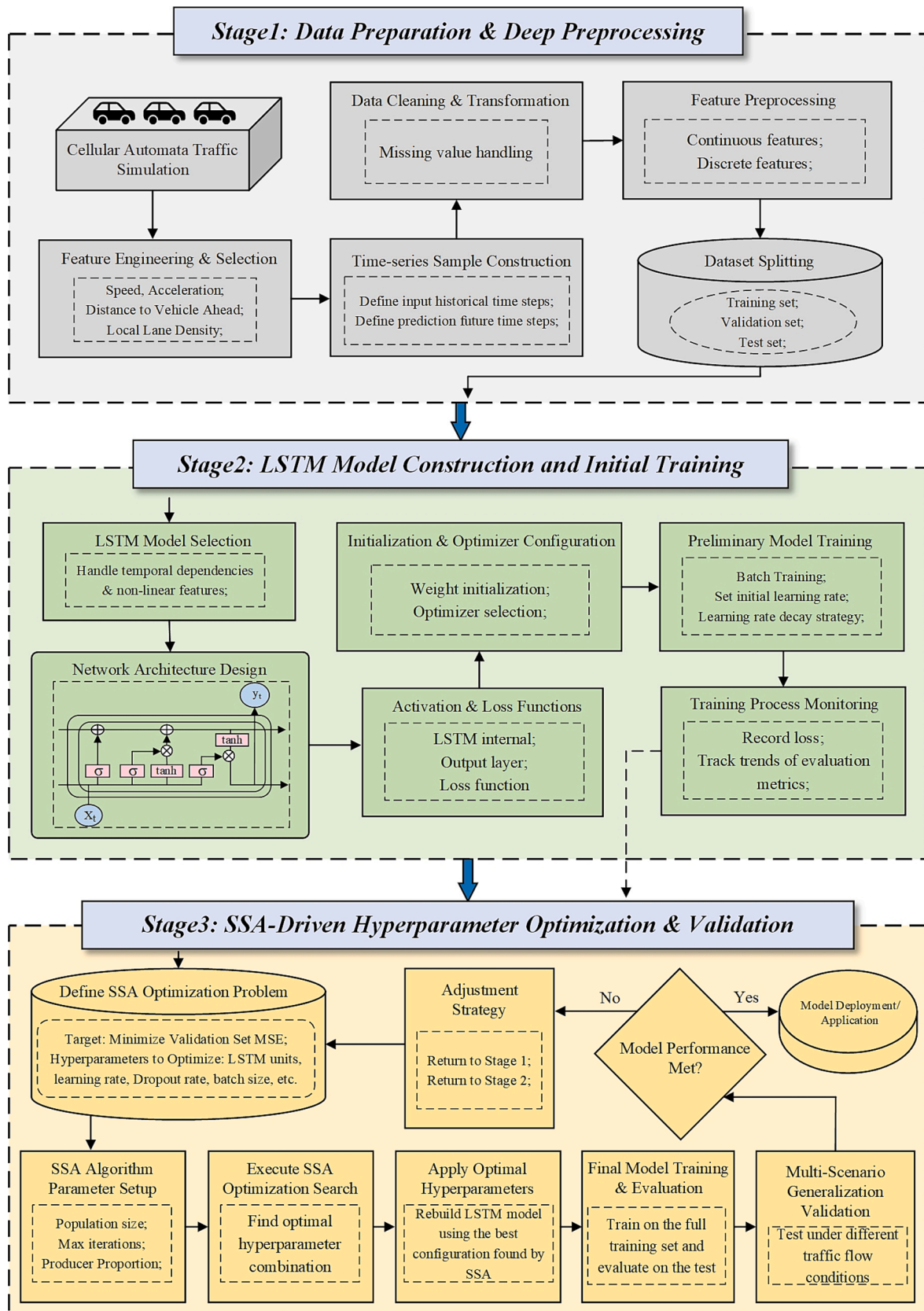


Fig. 3. Overall design framework structure.

constructing a traffic speed-following distance mapping graph, demonstrating the system's ability to operate stably in high-density scenarios.

More detailed explanations of the system design will be given below presented in Fig. 4; the experimental design framework proposed in this part is based on a multilevel and feedback structural design combining modelling, prediction and control, which is suitable for the study of automatic driving control systems in complex urban road environments and achieves the dual optimisation goals of traffic efficiency and driving safety by effectively integrating various modules, providing solid technical support for subsequent experimental validation and practical application.

As shown in the optimisation system model diagram, in the initialisation phase, the system is responsible for constructing the basic elements of the simulation environment, including parameters such as the required road structure, vehicle type, traffic density and duration. In the modelling and scheduling module, the system is based on the cell-automaton class, which advances the system state in time steps during the core simulation scheduling phase, controls the state update and interaction processing of all vehicles, and manages the meta cell update logic and vehicle behaviour execution. At each time step, the evolution of the system state is controlled, vehicle behaviours are advanced sequentially, intersection conflicts are handled, and state updates are executed. Eventually, the system will record data and visualise the results. During the simulation, traffic states, vehicle information and system metrics will be exported and recorded through image frames and data files and visualised through a graphical interface or animation frames. In the SSA-LSTM model, the trained LSTM model analyses the input traffic flow parameters as well as environmental and time step data. Then, after completing the speed prediction, the smart self-driving car can adjust its speed independently to achieve optimal speed and traffic efficiency. The data is then fed into the ACC algorithm for optimal evaluation of the following distance and control output.

#### 4.2. LSTM algorithm principles

LSTM is a special kind of Recurrent Neural Network (RNN). The basic units include a forgetting gate, an input gate and an output gate, which regulate the influence weights of historical information in the current state. LSTM can retain the key behavioural patterns through the long-term memory units, which gives it a natural advantage when dealing with the prediction of vehicle speeds, which is a problem of behavioural inertia and trend evolution. The input part of the model consists of the sliding window samples output from the simulation system in the previous section. Each input sample represents the set of behavioural states of a vehicle over  $n$  consecutive time steps, denoted as:

$$\mathbf{X} = [\mathbf{x}_{t-n+1}, \dots, \mathbf{x}_t] \in \mathbb{R}^{n \times d} \quad (3)$$

The above equation  $d$  represents the feature dimension, which includes variables such as speed, acceleration, vehicle type (using solo thermal coding), distance to the vehicle ahead, lane number, and local lane density. The output is a sequence of speeds over the next  $\tau$  time steps:

$$\mathbf{y} = [v_{t+1}, v_{t+2}, \dots, v_{t+\tau}] \in \mathbb{R}^{\tau} \quad (4)$$

The system standardises all continuous variables to prevent scale inconsistencies from interfering with model training. Discrete variables are then uniformly transformed into vectors through embedding layers or solo thermal coding to ensure the consistency of input features in the numerical space as visualized in Fig. 5.

Suppose that the input of the historical traffic flow sequence is denoted as  $\mathbf{x} = (x_1, x_2, \dots, x_T)$ , where  $T$  is the prediction period, the hidden state of memory block  $\mathbf{h} = (h_1, h_2, \dots, h_T)$ , and then the real output sequence  $\mathbf{y} = (y_1, y_2, \dots, y_T)$  can be iteratively calculated by following the equations (Kang et al., 2017):

$$y_t = W_{hy}h_t + b_y \quad (5)$$

$$h_t = H(W_{xh}x_t + W_{hh}h_{t-1} + b_h) \quad (6)$$

Where  $W$  denotes weight matrices (e.g.  $W_{xh}$  is the input-hidden weight matrix),  $b$  denotes bias vectors, and  $H$  is the hidden layer function, which can be computed in the following formulas:

$$i_t = \sigma(W_{xi}x_t + W_{hi}h_{t-1} + W_{ci}c_{t-1} + b_i) \quad (7)$$

$$f_t = \sigma(W_{xf}x_t + W_{hf}h_{t-1} + W_{cf}c_{t-1} + b_f) \quad (8)$$

$$c_t = f_t c_{t-1} + i_t g(W_{xc}x_t + w_{hc}h_{t-1} + b_c) \quad (9)$$

$$o_t = \sigma(W_{xo}x_t + W_{ho}h_{t-1} + W_{co}c_t + b_o) \quad (10)$$

$$h_t = o_t h(c_t) \quad (11)$$

The  $i$ ,  $f$ ,  $o$ , and  $c$  are the input gate, forget gate, output gate and activation vectors, respectively. Where  $\sigma(\cdot)$  is the standard logistic sigmoid function defined in the following formula:

$$\sigma(x) = \frac{1}{1 + e^{-x}} \quad (12)$$

$$h(x) = \frac{2}{1 + e^{-x}} - 1 \quad (13)$$

In addition, in model training, this study combined the practical

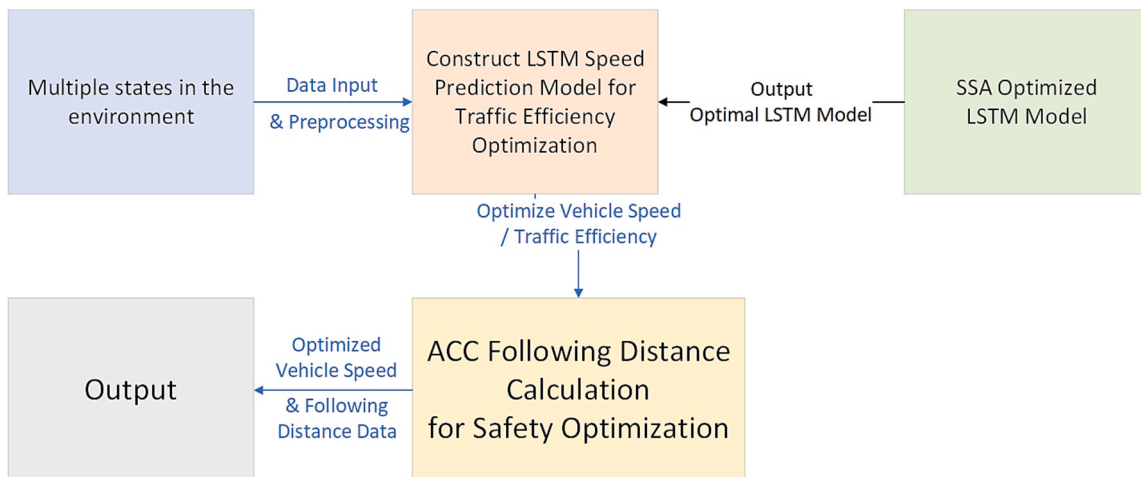


Fig. 4. Autonomous Driving Optimisation System Module.

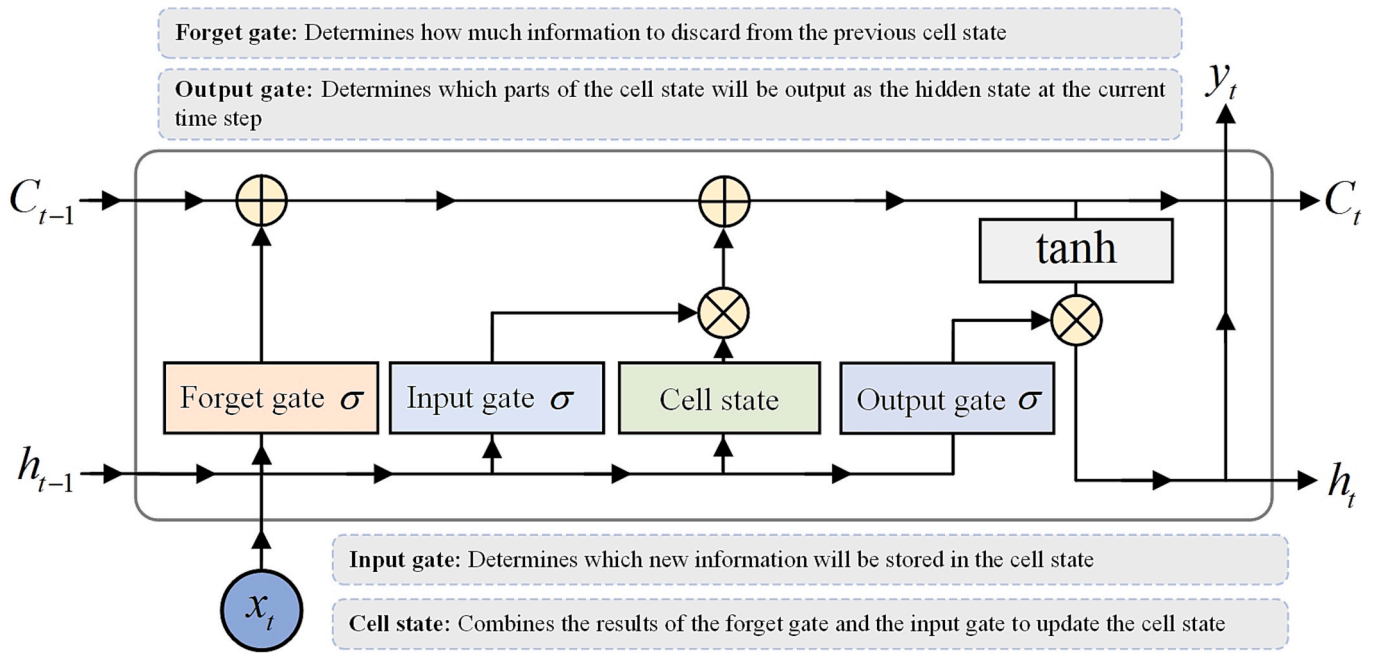


Fig. 5. Legend of LSTM neural network module form.

adjustment experience in the experiments. For example, when dealing with some of the vehicle samples in the simulation system with short trajectory life cycles, a sample screening mechanism was adopted to retain only the data whose history lengths meet the minimum time window requirement to ensure the consistency of sample quality. During this period, a training log recording function was set up in the multiple iteration phase of the model to track the trend of the loss function value, training error and validation error and ultimately determine the saving node of the optimal model in each experimental scenario. It is worth noting that the model training strategy is not fixed. In several experimental scenarios, this study made adaptive adjustments to the training strategy. For example, when dealing with the “interference complex” working condition data, the model’s initial training performance fluctuates a lot, and then by combining the strategies of reducing the learning rate, increasing the number of training rounds, and decreasing the length of the time step, the stability of the model is significantly improved. Similarly, in the “congestion impact” scenario, due to the drastic speed change, the relative speed feature dimension was added to enhance model performance in high-variation scenarios between vehicles. The programme extended the early stopping judgement window in the late stage of training to obtain smoother prediction results.

#### 4.3. SSA algorithm principles

The optimisation idea of SSA is based on the “discoverer-joiner” structure. One part of the individuals undertakes the task of global search (the discoverer) and continuously moves to a better position to find the optimal solution for fitness (Xue and Shen, 2020).

Individuals in the population update their positions according to the pheromone guidelines and adaptive strategies. In this experiment, the SSA algorithm is embedded into the LSTM model construction process and acts as an “external optimiser” to jointly tune the network structure and training parameters. Specifically, each SSA individual corresponds to a complete parameter combination used to construct an LSTM model and complete a full training process. Subsequently, the system evaluates the model performance on the validation set. It takes the mean square error as the fitness value of the combination, which is fed into the optimisation algorithm for the next-generation search.

In order to achieve this integration process, the system designs an

automated training and evaluation framework: SSA generates multiple individuals in each iteration, and the parameter combinations of each individual are dynamically injected into the training script; the system calls the model training module to complete the whole process, and feeds the results back to the SSA main program. In each iteration, the current optimal individual is retained, and the structure of discoverers and joiners is updated; all model training processes are enabled with the logging function for later retrospection and comparison. In the actual deployment process, the first step is to determine the core parameters to be optimised, including the number of LSTM layers (determining the depth of the model), the number of hidden units in each layer (affecting the expressive ability of the model); the length of the time window of the input samples (determining the coverage of the temporal information); the initial learning rate and the size of the training batch (affecting the efficiency of the training and the path of convergence); and the output prediction step size (determining the type of prediction task). The system automatically generates the initial population, and the range is set based on prior experience. The program set the maximum number of iterations during the training to ensure the search efficiency and convergence speed. It introduced an early stop mechanism to avoid the waste of resources caused by long-time training. For different traffic scenarios, the study deploys different optimisation tasks.

The hyperparameters that SSA will optimise are: LSTM cells, learning rate, dropout rate, batch size, etc. In detail, The SSA algorithm optimises the size of the hidden layer during the process of optimising hyperparameters, finding the optimal value. This enhances the model’s fitting ability, allowing it to capture the complex relationships of traffic flow more effectively and achieve the goal of optimizing vehicle speed and density. When optimising using a parameter matrix, overfitting may occur. To avoid overly conforming to the results obtained from the first optimisation calculation, the role of the SSA algorithm is to match to achieve the optimal effect automatically.

Additionally, the SSA algorithm optimises weight parameters. The parameter matrix is initially random and must be gradually optimised through training, but it may become trapped in a local optimum during the optimisation process. The SSA algorithm effectively helps the model escape from a local optimum state and find the global optimum combination, which is a significant advantage of SSA.

The SSA algorithm optimizes the LSTM network hyperparameters

through three distinct behavioural mechanisms, inspired by sparrow foraging and anti-predation behaviours. The algorithm effectively balances global exploration and local exploitation capabilities, making it particularly suitable for complex traffic flow prediction tasks. The global search capability of SSA helps avoid local optima that traditional optimisation methods often encounter when tuning neural network parameters.

According to the biological characteristics and foraging behaviours of sparrows, the specific calculation steps of the SSA algorithm are as follows (Li et al., 2022; Xue and Shen, 2020):

- (1) Discoverer Position Update: Discoverers typically have high energy reserves and are responsible for finding food sources for the entire population. Their position update formula is:

$$X_{ij}^{t+1} = \begin{cases} X_{ij}^t \cdot \exp\left(\frac{-i}{\alpha \cdot \text{iter}_{\max}}\right) & \text{if } R_2 < ST \\ X_{ij}^t + Q \cdot L & \text{if } R_2 \in [GRTEQT, ST] \end{cases} \quad (14)$$

where  $X_{ij}^t$  represents the position of the  $i$ -th sparrow in the  $j$ -th dimension at the  $t$ -th iteration,  $\alpha \in [0, 1]$  is a random number,  $\text{iter}_{\max}$  is the maximum number of iterations, and  $R_2$  and  $ST$  represent the alarm value and safety threshold, respectively.

- (2) Follower Position Update: Followers monitor the behaviour of discoverers and compete for food resources. When followers have poor fitness, they need to forage elsewhere:

$$X_{ij}^{t+1} = \begin{cases} Q \cdot \exp\left(\frac{X_{\text{worst}}^t - X_{ij}^t}{i^2}\right) & \text{if } i > n/2 \\ X_p^{t+1} + |X_{ij}^t - X_p^{t+1}| \cdot A^+ \cdot L & \text{otherwise} \end{cases} \quad (15)$$

where  $X_p$  is the optimal position occupied by the discoverer,  $X_{\text{worst}}$  denotes the current global worst location, and  $A^+ = A^T (AA^T)^{-1}$ .

- (3) Scout Position Update: Scouts are responsible for monitoring danger and guiding the population to avoid risks. When scouts become aware of danger, their position update formula is:

$$X_{ij}^{t+1} = \begin{cases} X_{\text{best}}^t + \beta \cdot |X_{ij}^t - X_{\text{best}}^t| & \text{if } f_i > f_g \\ X_{ij}^t + K \cdot \frac{|X_{ij}^t - X_{\text{worst}}^t|}{(f_i - f_w) + \epsilon} & \text{if } f_i = f_g \end{cases} \quad (16)$$

where  $X_{\text{best}}$  is the current global optimal location,  $\beta$  is the step size control parameter, and  $f_i$ ,  $f_g$ ,  $f_w$  represent the current individual, global best, and worst fitness values, respectively.

Through these three behavioural mechanisms, the SSA algorithm effectively optimises the LSTM hyperparameters, including hidden layer dimensions, learning rates, and network depth, enabling the model to capture complex traffic flow patterns more effectively and achieve superior prediction performance in vehicle speed and density optimization tasks.

SSA optimisation significantly improves the experimental results. Compared with the Unoptimised model, the hyperparameter combinations found by SSA generally show lower average values of validation and testing errors, especially in the interference complex scenario. The optimised model can better sense the sudden change in speed trend while maintaining a compact and synchronised state.

In summary, the sparrow search algorithm serves as the core support for optimising the LSTM model structure in this study, and its global exploration capability and local refinement mechanism provide a double guarantee of stability and efficiency for the model parameter tuning process. In complex traffic behaviour modelling, replacing manual debugging using automated parameter learning improves the accuracy

of the predictive model and enhances its cross-scenario deployment capability, which is one of the indispensable optimisation tools for realising large-scale intelligent traffic modelling (Li et al., 2025).

## 5. ACC for safe distance regulation

Adaptive cruise control (ACC) technology significantly improves the stability and efficiency of the traffic flow by ensuring safety by adjusting the vehicle's speed and distance from the vehicle in front in real-time. The combination of ACC technology and CA models can more accurately simulate the dynamic changes of the queuing vehicles, thus providing strong support for developing efficient traffic management strategies. This study proposes a cellular automata (CA) model for mixed traffic flows that considers the driving behaviour of vehicles in a queue of automated vehicles (Jiang et al., 2021). In recent years, the application of ACC technology in intelligent networked vehicles has become increasingly popular, and its integration with traffic flow modelling has significantly enhanced the efficiency of urban road access.

The structural design of the adaptive cruise control strategy relies on a multi-module parallel collaboration mechanism. The control framework is divided into three functional layers: the prediction and perception layer, the control and decision-making layer, and the execution and regulation layer, each operating in real-time through data channels and feedback mechanisms. The overall structure is designed to combine the prediction output with the current state information of the vehicle and the vehicle in front of it to generate control commands for future evolutionary trends (Yang et al., 2024).

As shown in the Fig. 6, adaptive cruise control systems usually respond with a fixed rule-based following model, such as setting a constant time headway or minimum spacing.

The first core function of the ACC module is calculate `safe_distance` (`front_speed`, `following_speed`), whose primary function is to calculate the required minimum safe following distance in real time according to the current vehicle speed and the speed of the vehicle in front. The final result is calculated as the maximum value between the sum of the two and the minimum set distance, thus ensuring the vehicle's safety under different speed conditions.

ACC can control vehicle acceleration or deceleration by calculating the minimum safe distance using the following formula. The formula is as follows:

$$d_{\text{safe}} = \max\left(d_{\min}, \tau \cdot v + \frac{(v - v_f)^2}{2a_c}\right) \quad (17)$$

where  $\tau$  is the ideal time headway,  $v$  is the local speed,  $v_f$  is the speed of the front vehicle, and  $a_c$  is the comfort deceleration threshold. If the current actual distance is lower than  $d_{\text{safe}}$ , the controller outputs negative acceleration; otherwise, it outputs acceleration.

The second core function is "calculate acceleration", which determines whether acceleration or deceleration is required based on the actual distance between the current vehicle and the vehicle in front, and the target speed. This ensures that the regulation behaviour is carried out within a comfortable range and that sudden acceleration or deceleration is avoided as much as possible.

The actuation tuning layer translates the acceleration values output from the controller into vehicle longitudinal drive control signals. It aligns them with the vehicle's physical constraints, including safety boundary settings such as maximum deceleration limits, lane change transition locks, and minimum cruise speeds. In addition, this layer is responsible for linking with the system safety and security mechanism to override the standard control signals and prioritise the execution of risk avoidance commands in emergencies.

From the perspective of control strategy evolution, the introduction of forward prediction capability is considered a key direction to enhance the performance of adaptive cruise control (ACC) performance. Based on the existing prediction model, which can predict the future vehicle speed

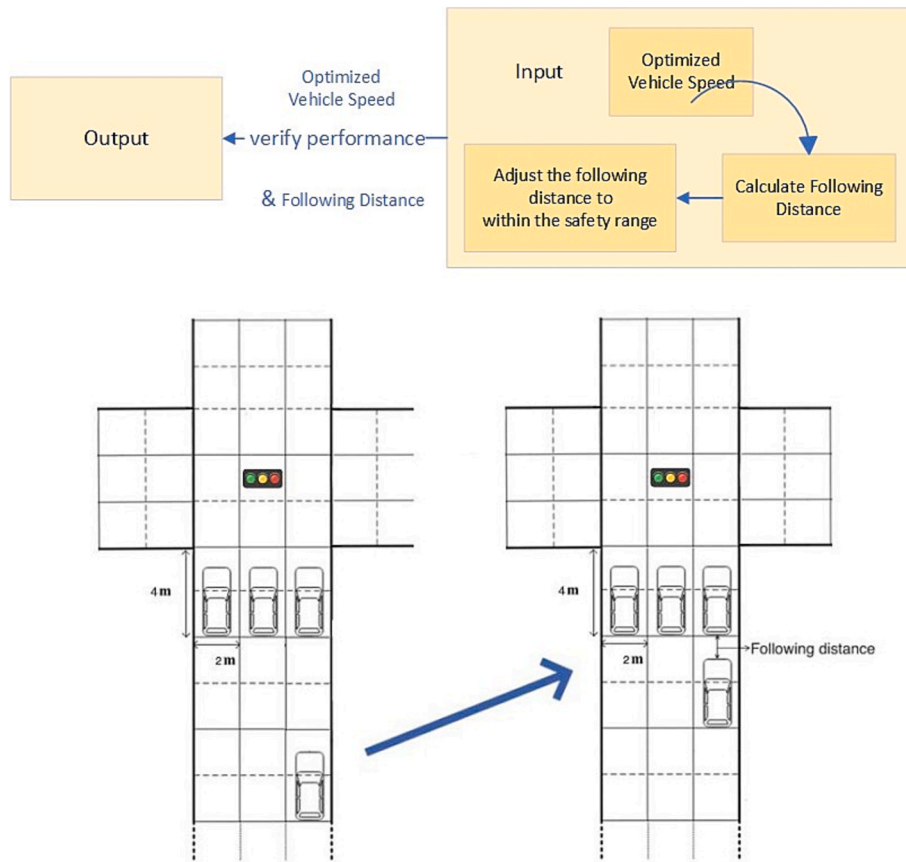


Fig. 6. Following distance planned by ACC.

sequence with short-term accuracy, constructing an adaptive cruise control strategy based on the prediction drive has the conditions for

realisation. This study proposes a cellular automata (CA) model for mixed traffic flows that considers the driving behaviour of vehicles in a

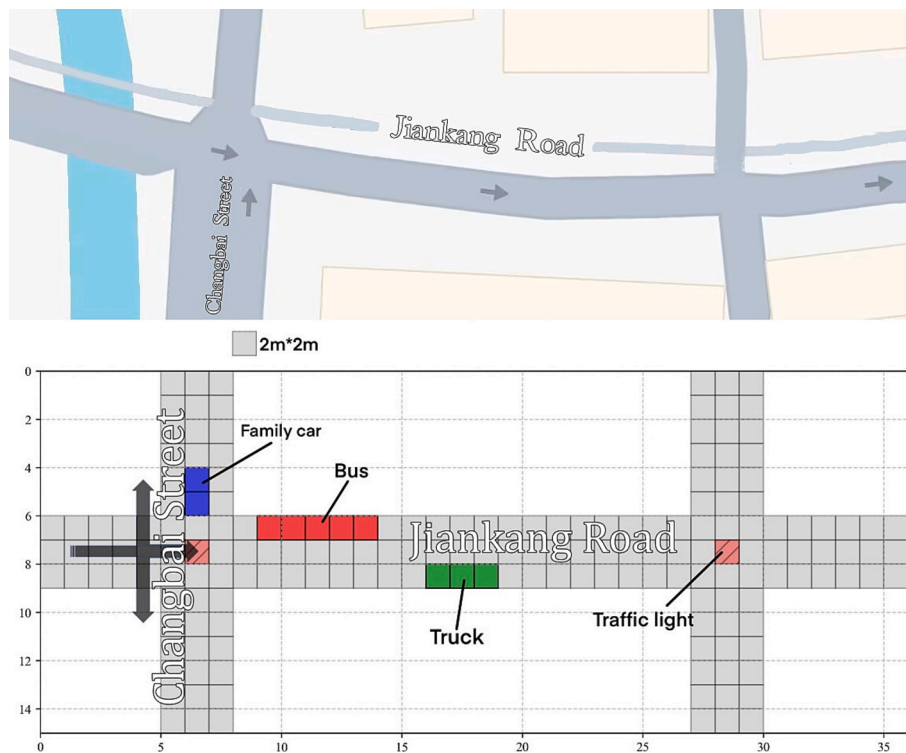


Fig. 7. The real scenario considered in the study.

queue of automated vehicles (Jiang et al., 2021). This control strategy aims to improve the vehicle response to complex dynamic scenarios and reduce unnecessary acceleration and deceleration impacts.

### 6. Case study region

In order to validate the performance of the control algorithm, a realistically existing road was chosen as the base reference for meta cellular automata modelling. As shown in the Fig. 7, the traffic simulation environment constructed in this study is sampled from a realistic and real-life urban intersection scenario, with a total length of about 70 m, containing a three-lane main road and a single-lane side road, forming an intersection for vehicles entering and exiting a residential area. This structure generally reflects the traffic flow relationship between urban residential areas and the main road, facilitating the analysis of congestion and following behaviour during peak hours. The core idea is to partition the road into regular cells, each representing a tuple, with the state of each tuple depending on whether it is occupied by a vehicle, which advances at a discrete speed, with each step guided by neighbourhood rules (Bonivento et al., 2011).

The state evolution of meta-cellular automata is updated based on discrete time steps. In each time step, the vehicle performs operations such as acceleration, deceleration, lane changing and following according to predefined rules. The classical NaSch model is extended in this study, to include the differences in physical parameters (e.g., length, maximum speed) of different types of vehicles, which include small cars, buses, and lorries, and introduce a dynamic lane-changing logic based on the state of the lanes in front of the vehicle to simulate more realistically the diversified traffic scenarios and to reflect the impact of vehicle length on road utilisation and capacity (Hu et al., 2024).

### 7. Results and discussion

To verify the modelling adaptability and execution robustness of the system in different traffic environments, three typical traffic experimental scenarios are designed in this paper:

*Experiment 1: Stable Passage Experimental environment.*

The simulation of a regular weekday morning traffic flow with moderate traffic density and unobstructed lanes is mainly used to test the system's basic stability under normal traffic conditions and the natural evolution of vehicle behaviour.

*Experiment 2: High-density congestion experimental environment.*

Simulate traffic during the morning and evening peak hours, set higher vehicle injection rates and a mixed environment with multiple types of vehicles, and shorten the inter-vehicle spacing in parallel to test the system's operability and state evolution patterns under high-density conditions. Increase the number of vehicles injected per unit of time and set some lanes for heavy vehicles to keep the system under high-load operation.

*Experiment 3: Verification of system stability in case of traffic accidents.*

Simulate the accident or temporary closure area, set some road units as "impassable," put the impassable unit in the middle of the main road, simulate the temporary closure of the road or the accident blocking the scene, observe the vehicles' detouring, deceleration, or blocking phenomenon during this period, and assess the system's adaptability to unexpected events and ability to deal with faults.

To ensure reproducibility and comprehensively elucidate the experimental setup, Table 1 summarizes all key parameters employed within the simulation system. This encompasses cellular automata modelling, SSA-LSTM optimisation, and adaptive cruise control configurations, alongside the parameter settings for the three experiments:

The parameter values listed in this table were selected based on practical considerations and experimental requirements. The 2-meter cell size provides adequate spatial resolution while maintaining computational efficiency, with vehicle type distributions (60 % cars, 20

**Table 1**  
Key parameters table.

Parameter Category	Parameter Name	Value	Description
Continued on next page			
	Cell Size	2 m	Basic discretization unit for road modeling
	Road Length	70 m	Total visible simulation area (60 cells)
	Vehicle Type Distribution	Cars: 60 % Trucks: 20 % Buses: 20 %	Probability distribution for vehicle injection
	Vehicle Cell Occupancy	Cars: 2 cells Trucks: 3 cells Buses: 5 cells	Spatial occupation for different vehicle types
	Speed Limit Range	30–60 km/h	Upper and lower bounds for vehicle operation
	Turning Probability	Straight: 50 % Right: 30 % Left: 20 %	Directional settings at three-lane intersection
	Vehicle Injection Rate	Exp. 1: 1 per 10 steps Exp. 2: 1 per 3 steps	Traffic flow settings for different scenarios
	Safety Distance Threshold	2 cells (4 m)	Minimum safe following distance
SSA-LSTM Parameters	Historical Time Window	10 steps	LSTM input sequence length
	Prediction Horizon	3 steps	Forward prediction time range
	Model Invocation Frequency	Every 1 step	Prediction module execution frequency
	Total Simulation Steps	1000 steps	Complete simulation cycle duration
	Discoverer Ratio	20 %	Producer proportion in SSA population
	Scout Ratio	10 %	Danger-aware individual proportion
	Safety Threshold (ST)	0.8	Danger detection critical value
	Population Size	100 individuals	SSA optimisation swarm size
	Maximum Iterations	1000	SSA optimisation termination condition
	LSTM Hidden Units	128	Bidirectional GRU hidden layer size
Feature Dimension	256	Final electrical feature vector dimension	
ACC Controller Parameters	Ideal Time Headway ( $\tau$ )	Variable	Time interval parameter in Equation (20)
	Comfort Deceleration ( $a_c$ ) Minimum Following Distance	Variable $\geq 2.90 m$	Threshold to avoid sudden braking Lower bound for actual safe distance
	Control Execution Frequency	Every time step	ACC algorithm response frequency
	Speed Regulation Range	Dynamic	Acceleration/ deceleration control magnitude
	Safety Boundary Settings	Max. deceleration limits	Physical constraints and safety limits

(continued on next page)

Table 1 (continued)

Parameter Category	Parameter Name	Value	Description
Experimental Scenario Parameters	Experiment 1: Stable Passage	Moderate density	Normal weekday morning traffic simulation
	Experiment 2: High-density Congestion	High injection rate	Morning/evening peak hour simulation
	Experiment 3: Traffic Accident	Road obstruction	Temporary closure scenario
	Accident Trigger Time	Step 300	Obstacle appearance moment in Exp. 3
	Independent Runs	30 trials	Statistical analysis sample size

% trucks, 20 % buses) reflecting a typical urban traffic composition. Speed limits of 30–60 km/h correspond to urban arterial road conditions. The 10-step historical window balances temporal context with computational complexity, while the 3-step prediction horizon provides sufficient foresight for proactive control. SSA population size of 100, combined with a maximum of 1000 iterations, ensures thorough optimisation without excessive computational overhead. Variable ACC parameters enable adaptive adjustment based on traffic conditions, with a minimum following distance of 2.90 m providing an adequate safety margin. Three distinct experimental scenarios (stable, congested, and accident) ensure statistical significance and reproducibility.

7.1. Stable passage experimental environment

The experiment developed a base access model for a three-lane linear

road intersection with a linear section of 60 cells (about 120 m) visible length, and the system was equipped with a unilateral injection port with a fixed injection frequency of 1 vehicle per 10 steps. The vehicles are initially set up with a 60 % probability of occurrence for family cars, 20 % for trucks and 20 % for buses. At three-lane intersections, the turning probabilities of vehicles are 50 % straight ahead, 30 % right turn, and 20 % left turn. The speed distribution is concentrated in the low and medium speed bands with upper and lower limits of 30–60 km/h. The total number of simulation steps is 1000.

As shown in the Fig. 8, the optimal control group records the vehicle operating state between the 20th and 25th seconds in six consecutive frames of the visualisation of the traffic flow in the stable passing experiment. Each rectangular grid in the figure represents a tuple; each tuple corresponds to a 2-metre road unit, and the colours indicate different types of vehicles, with blue indicating family cars, green indicating trucks, and red indicating buses. It can be seen from the images that the vehicle presence rate is evenly distributed. There is no traffic jam in the visible area, indicating that the autonomous vehicle has a stable speed trend, the following rhythm is consistent, no local braking or stopping occurs, and the rear of the convoy can complete the speed synchronisation quickly. This visual continuity visualises the role of the predictive controller.

The control group adopts the traditional rule-based control based on vehicle distance difference. In contrast, the optimisation group introduces the LSTM model of SSA optimisation for predicting speed in the next three steps. The prediction module is invoked once every 1 step and extracts the historical speed sequence of 10 steps through a sliding window as the input. The output sequence is handed over to the controller to judge whether to accelerate or decelerate ahead of time after the trend analysis to generate the target speed.

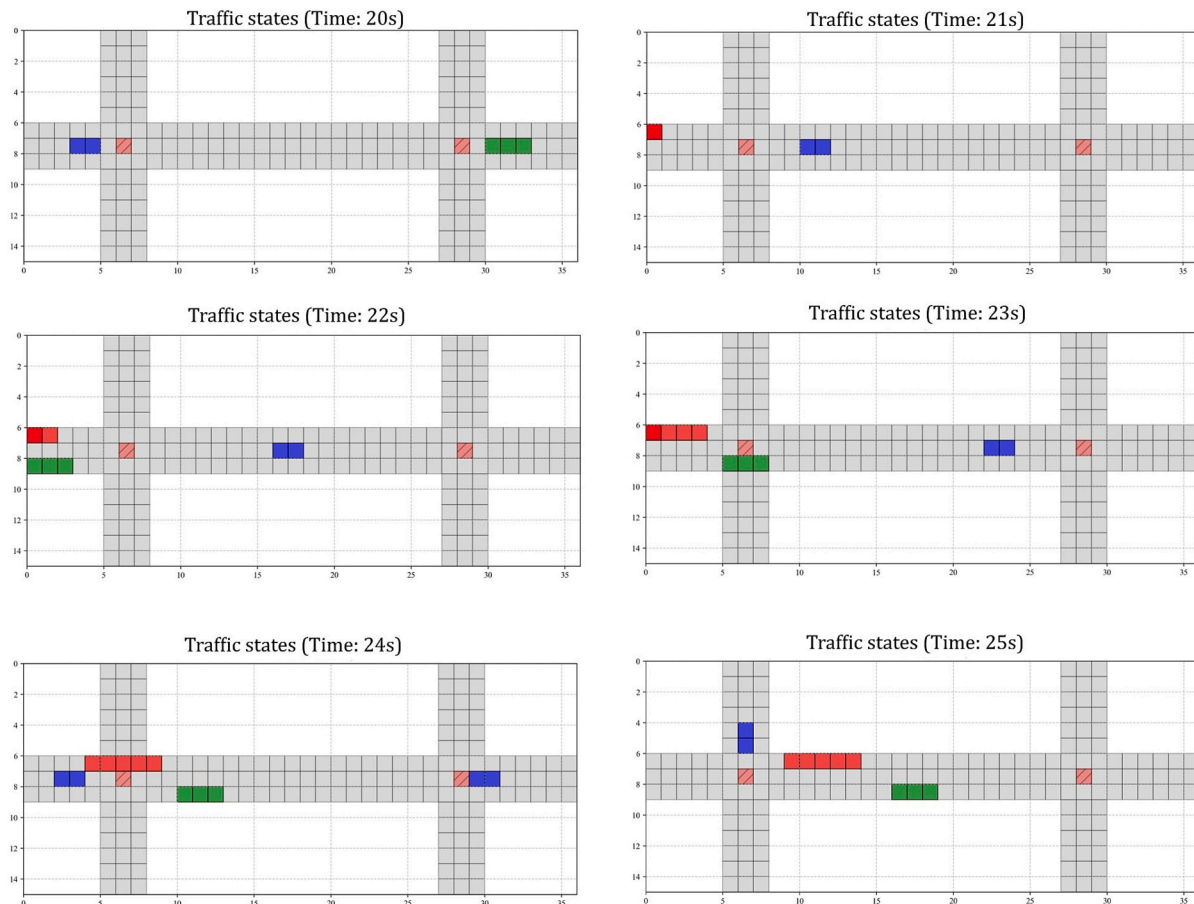


Fig. 8. CA simulated traffic states in Experiment 1 (sec 20–25).

This study also provides numerical statistics on the speed and following distance of the vehicle during travelling based on the time series recorded by the system and as recorded in Table 2.

To quantify the differences in vehicle behaviour further, the following Fig. 9, “Vehicle speed comparison before and after SSA-LSTM optimisation,” shows the curves of the vehicle speed changes, comparing the vehicle speed distribution under different control strategies.

The graph's vertical axis represents the vehicle speed, and the horizontal axis represents the time; the red solid line represents the control group; the green solid line represents the optimisation group; the red dashed lines mark the upper and lower limits of the vehicle speed. It can be observed that the speed curves of the vehicles in the control group show high-frequency fluctuations, with multiple sharp folding points, reflecting frequent acceleration and deceleration of the vehicles in a short period, with a higher frequency of low-speed occurrences, suggesting the existence of more discontinuous behaviours, such as braking and starting, etc.; whereas, the speed fluctuations of the vehicles in the optimisation group are small, mainly focusing on the middle and high-speed intervals, and the speed curves are much smoother, with almost no mutation points. The vehicle operation discontinuity is significantly enhanced. Calculated from the graphs, the average speed of the optimised group increased by 3.89 % compared to the control group.

It is worth noting that, as shown in the image, there was a noticeable increase in the final stage of the simulation experiment (between 55 and 60 min). This increase was also observed in subsequent images, so it is explained here for consistency.

This change occurred in the traffic flow simulation due to the characteristics of traffic flow. During the CA simulation, since the CA simulation must be completed within a limited timeframe, all vehicles must exit the simulation by the end of the simulation. As a result, boundary effects are more likely to occur toward the end of the simulation.

Additionally, since the experiment employs the LSTM algorithm as a predictive tool, and the LSTM algorithm relies on historical sequence modelling, requiring data from both preceding and subsequent periods as support, at the end of the experiment, near the simulation boundary, the behaviour pattern of concentrated vehicle departures differs significantly from steady-state traffic patterns. This results in the final data becoming out-of-distribution samples. Consequently, the LSTM algorithm may exhibit phenomena resembling acceleration due to insufficient generalisation capabilities.

This study also provides numerical statistics on the speed and following distance of the vehicle during travel based on the time series recorded by the system. The results show that the speed of the optimised autonomous vehicle is significantly increased. As shown in the Fig. 10, the speed of each vehicle has shifted from the low-speed range to the high-speed range after the optimisation. The concentration area of the speed data is reflected in the y-axis values where the dense areas in the picture are located. The speed data of each vehicle has improved after the optimisation:

**Table 2**  
Speed comparison data in experiment 1.

Time [minutes]	Un-optimised Speed [km/h]	Optimised Speed [km/h]	Improvement [%]
5	42,89	44,71	4,24
10	43,41	45,24	4,23
15	43,08	45,08	4,66
20	43,51	45,24	3,97
25	43,10	44,83	4,01
30	43,44	45,24	4,16
35	43,13	44,95	4,22
40	43,21	45,11	4,41
45	43,34	44,89	3,59
50	43,41	45,16	4,02
55	43,56	44,90	3,07
60	47,11	48,10	2,09

The speed standard deviation statistics can be used as an important reference indicator of behavioural stability throughout the vehicle's cycle. The data showed that the speed standard deviation of all vehicles in the optimisation group was generally lower than that of the control group, with a reduction of approximately 67 %. This indicates that the predictive control reduces unnecessary acceleration and braking behaviours while maintaining the target speed, which reduces the degree of speed fluctuation and results in a smoother operation, significantly improving the stability of the operation and the comfort of the ride. Vehicles were able to complete speed convergence faster after joining the fleet, reducing unnecessary acceleration and deceleration manoeuvres. This conclusion can be verified by the graphical data presented in Table 3 and Table 4.

According to the graphical data statistics, the average following distance of the optimisation group was 3.01 m during the simulation cycle, while that of the control group was 2.83 m, an increase of 6.06 %. Meanwhile, the minimum distance remained above 2.90 m without triggering the safety threshold warning. Most of the vehicles had a minimum distance much higher than the set 2-cell safety threshold and the minimum following distance increased by 2.37 % compared to the control group. By analysing the minimum distance, average distance and distance volatility between the vehicle and the vehicle in front during the simulation cycle, it is found that the standard deviation of the following distance is 5.87 % lower than that of the control group, which reflects the system's effective control of the safety distance, as well as rhythmic consistency and smooth behaviour. It shows that the system has good regulation ability in micro-safety. The trend suggests that under predictive control, the vehicle is able to develop a more consistent following rhythm, thus reducing the risk of tailgating compression.

In the data analysis of following distance, the optimisation group demonstrates a more stable and safe following distance judgement when the traffic flow changes. The control principle is that the vehicle queue forms a continuous cyclic rhythm of injection and discharge during the system operation. In the control group, the vehicles usually have a delayed response after a slight deceleration of the vehicle in front of them, which can easily lead to a short-term “zip effect”, i.e., a chain reaction of local acceleration and deceleration. In the optimisation group, the controller obtains the speed trend information in advance, and the vehicle behaviour can be fine-tuned in advance, thus avoiding the rhythm break and forming a more stable operating rhythm. As a result, the following distance is well controlled regardless of whether the vehicle speed is accelerated or decelerated in the traffic flow, and the average following distance is improved by 5.47 %. Detailed data is shown in Table 5:

Fig. 11 shows the “Optimised speed – Following distance”; the vertical axis represents the vehicle speed, the horizontal axis represents the time; the blue solid line represents the current vehicle speed, and the red dotted line represents the current following distance. It can be seen that the following distance curve always maintains within the safe following range. This feature suggests that the predictive support mechanism improves the speed's stability. In addition, the synergistic change of speed and following distance also shows that the vehicle speed can quickly keep in line with the surrounding vehicles after entering the queue without any noticeable jitter or sudden change, reflecting the controller's good ability to regulate the rhythm of the traffic flow.

The stable passage experiment verifies the ability of the predictive drive control strategy to optimise the vehicle operating state without external perturbations. Vehicle behaviours show better continuity and consistency in time and space, and the system effectively suppresses speed and distance fluctuations and improves the overall coordination of traffic operation through trend identification and front-loaded regulation mechanisms.

### 7.2. High-density congestion experimental environment

This experiment simulates the high-density traffic conditions during

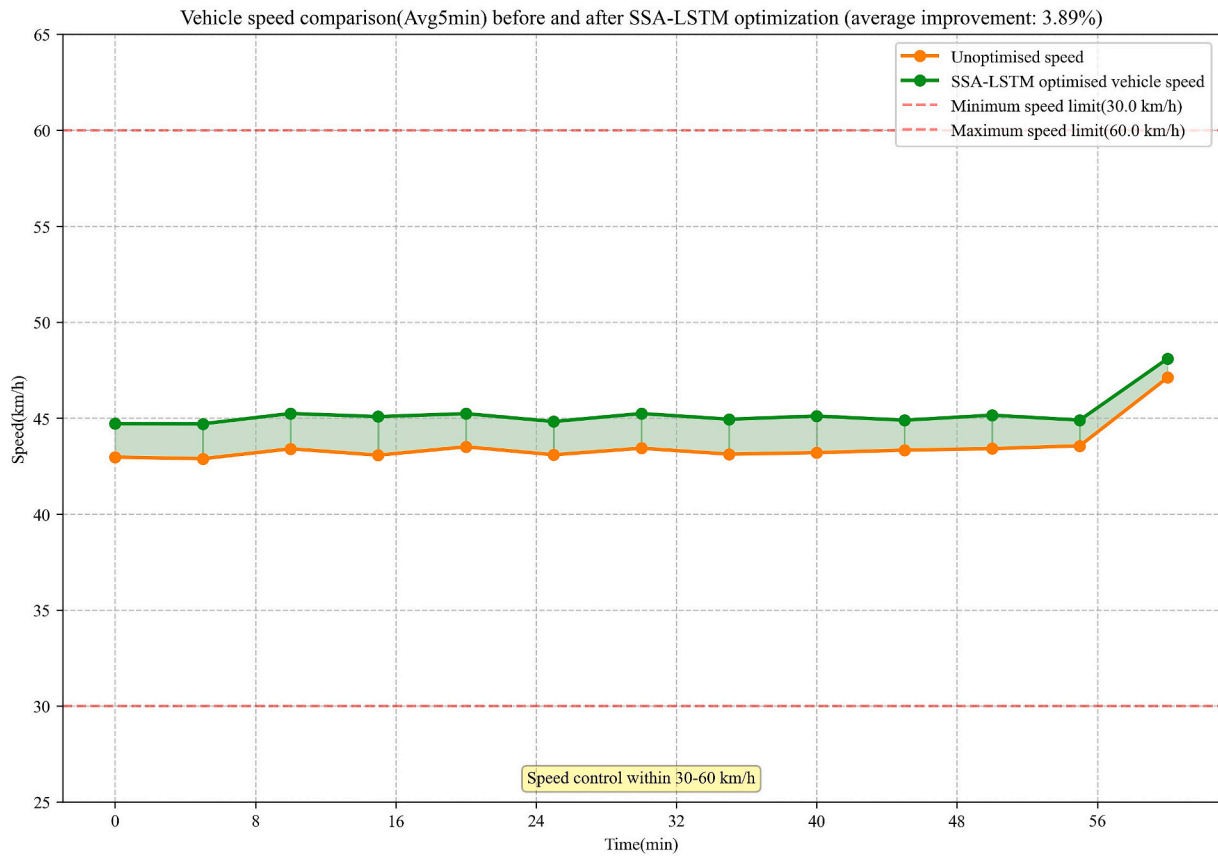


Fig. 9. Comparison of vehicle speed before and after optimisation in Experiment 1.

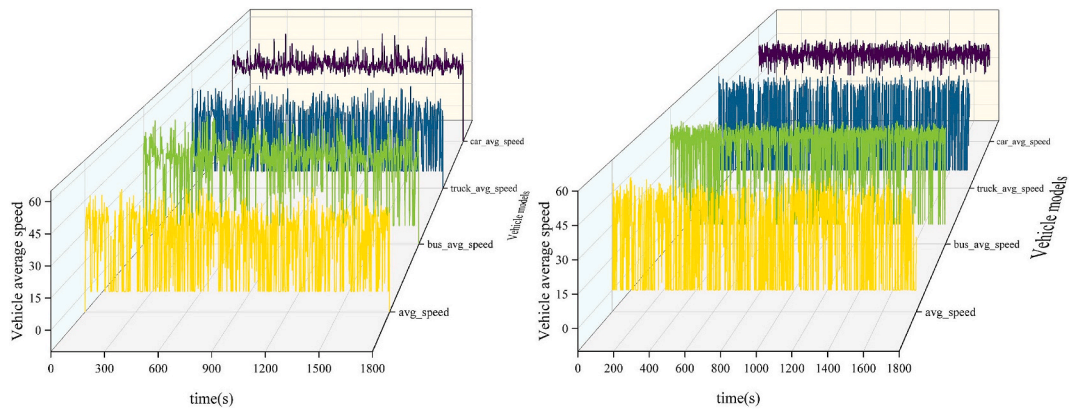


Fig. 10. Speed data for different models before and after optimisation in experiment 1.

**Table 3**  
Vehicle speed STD in experiment 1.

Vehicle	Speed STD ( $\sigma$ )
Un-optimised Speed (km/h)	1,09
Optimised Speed (km/h)	0,88
Improvement (%)	67

**Table 4**  
Distance analysis in experiment 1.

Vehicle	Un-optimised Distance [m]	Optimised Distance [m]	Improvement [%]
Minimum Distance	2,83	2,90	2,37
Average Distance	2,83	3,01	6,06

the morning and evening peak periods. It investigates the control strategy's reaction speed, deceleration smoothness and overall traffic flow stability under sudden congestion and a sharp decrease in vehicle speed. Under the premise of keeping the road structure and vehicle type probability unchanged, the vehicle injection frequency is increased to 1 vehicle every three steps. The traffic flow impact detection is performed

after 400 consecutive injection steps, and the actual vehicle density is close to the upper limit of the road capacity. Meanwhile, the system in the experimental setup randomly triggers a forced deceleration event (speed plunge of no more than three units) of the front vehicle every 200

**Table 5**  
Following distance comparison data in Experiment 1.

Time [minutes]	Un-optimised distance [m]	Optimised Distance [m]	Improvement [%]
30	2,83	2,89	1,92
35	2,83	2,90	2,37
40	2,83	2,99	5,35
45	2,83	2,93	3,43
50	2,83	2,96	4,51
55	2,83	2,92	2,87
60	2,83	3,34	17,84

steps to simulate potential congestion triggers, forcing the vehicle to decelerate and forming a flow bottleneck; all vehicles are modelled with the same structure, with an initial speed of 3 units/step and the maximum speed of 5 units/step, to observe the timing of the intervention of the rear-end vehicle's control response and magnitude of the effect. The control group continued to use the rule-based control approach, while the optimisation group predicted trends in real time through the LSTM model and fed the results back to the controller. The total number of steps in the simulation is 1000, and the prediction module is invoked once per step to extract the historical 10-step speed sequence and predict the future 3-step speed trend. The controller calculates the velocity change slope based on the prediction results and determines whether to execute the deceleration operation in advance.

As shown in the Fig. 12, the CA simulated traffic state map demonstrates a visual snapshot of the optimisation group during the peak congestion period, covering a sequence of frames between the 495th and 500th seconds. The figure shows that despite the obvious area of dense vehicle stacking ahead of the entering road, the optimal control strategy allows the following vehicles to generally complete the speed buffer before the preceding vehicle has dramatically decelerated, thus effectively avoiding the transmission of large-scale fluctuations. Overall, there did not appear to be congestion, although the roads were busy due

to the increased injection of vehicles.

In Experiment 2, numerical statistics of the vehicle's speed and following distance during travelling were carried out based on the time series recorded by the system. The results are shown in Fig. 13. The speed of the optimised autonomous vehicle was significantly increased, with an average speed increase of 4.2 % compared to the control group with the traditional control method and demonstrated with data shown in Table 6.

In the image of "Vehicle speed comparison before and after SSA-LSTM optimisation" in Experiment 2, the curves of vehicle speed changes are shown to compare the distribution of vehicle speeds under different control strategies. The vertical axis represents the vehicle speed, the horizontal axis represents the time, the red solid line represents the control group, the green solid line represents the optimisation group, and the red dashed lines mark the upper and lower limits of the vehicle speed. In Experiment 2, the speed curves of the vehicles in the control group showed higher frequency fluctuations, reflecting frequent acceleration and deceleration of the vehicles in a short period. In contrast, the speed fluctuations of the vehicles in the optimisation group were more minor, mainly focusing on the middle and high-speed intervals. The speed curves were smoother, with a significantly greater continuity of the vehicle operation. From the perspective of the behavioural trajectory, most of the vehicles in the optimisation group completed the transition with a lower slope, reflecting the advantages of advanced and rhythmic regulation of predictive driving.

Fig. 14 clearly shows that the passing speeds of all types of vehicles in the optimised group have been effectively increased; the recorded speed data shows that the speeds have increased from the low-speed range before optimisation to within the high-speed range after optimisation, this information can be observed by the concentrated area of data in the figure:

Fig. 15 shows the relationship between "Optimised speed – Following distance", where the vertical axis represents the speed of the

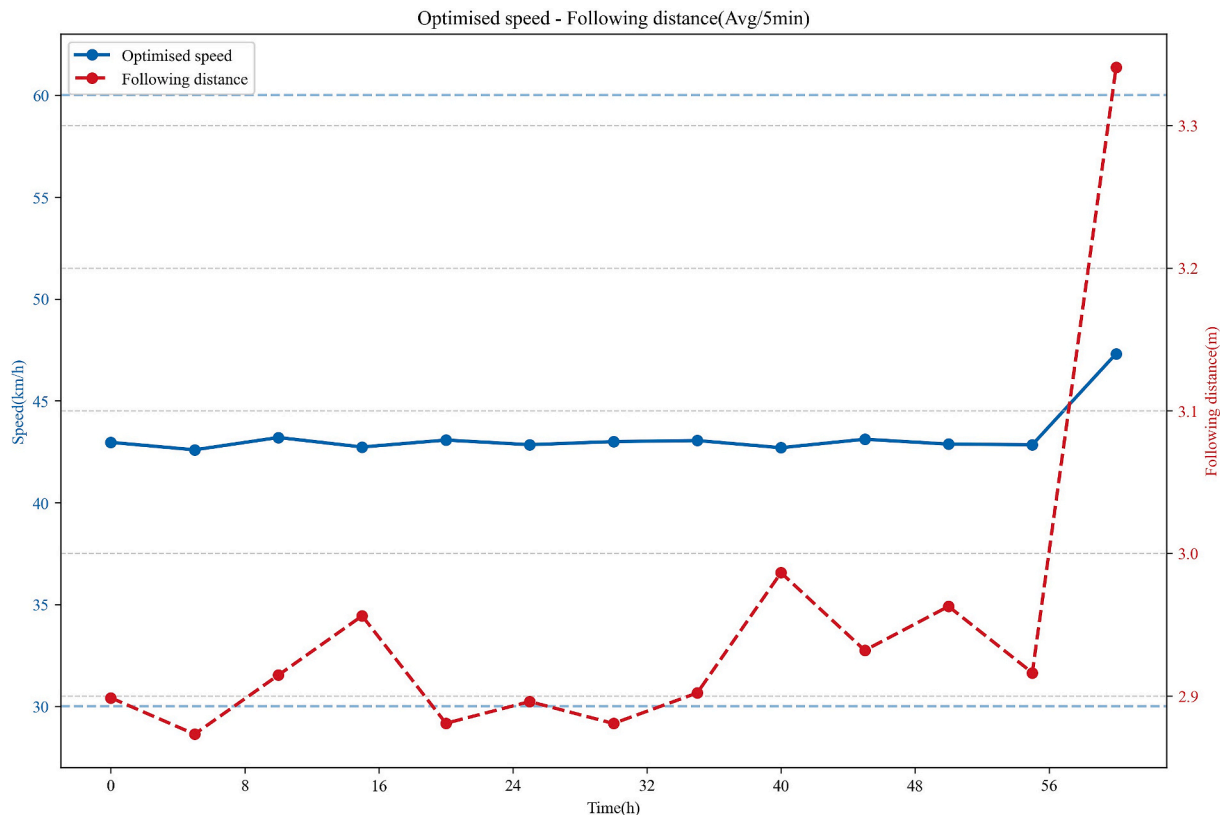


Fig. 11. Vehicle speed versus following distance after optimisation in experiment 1.

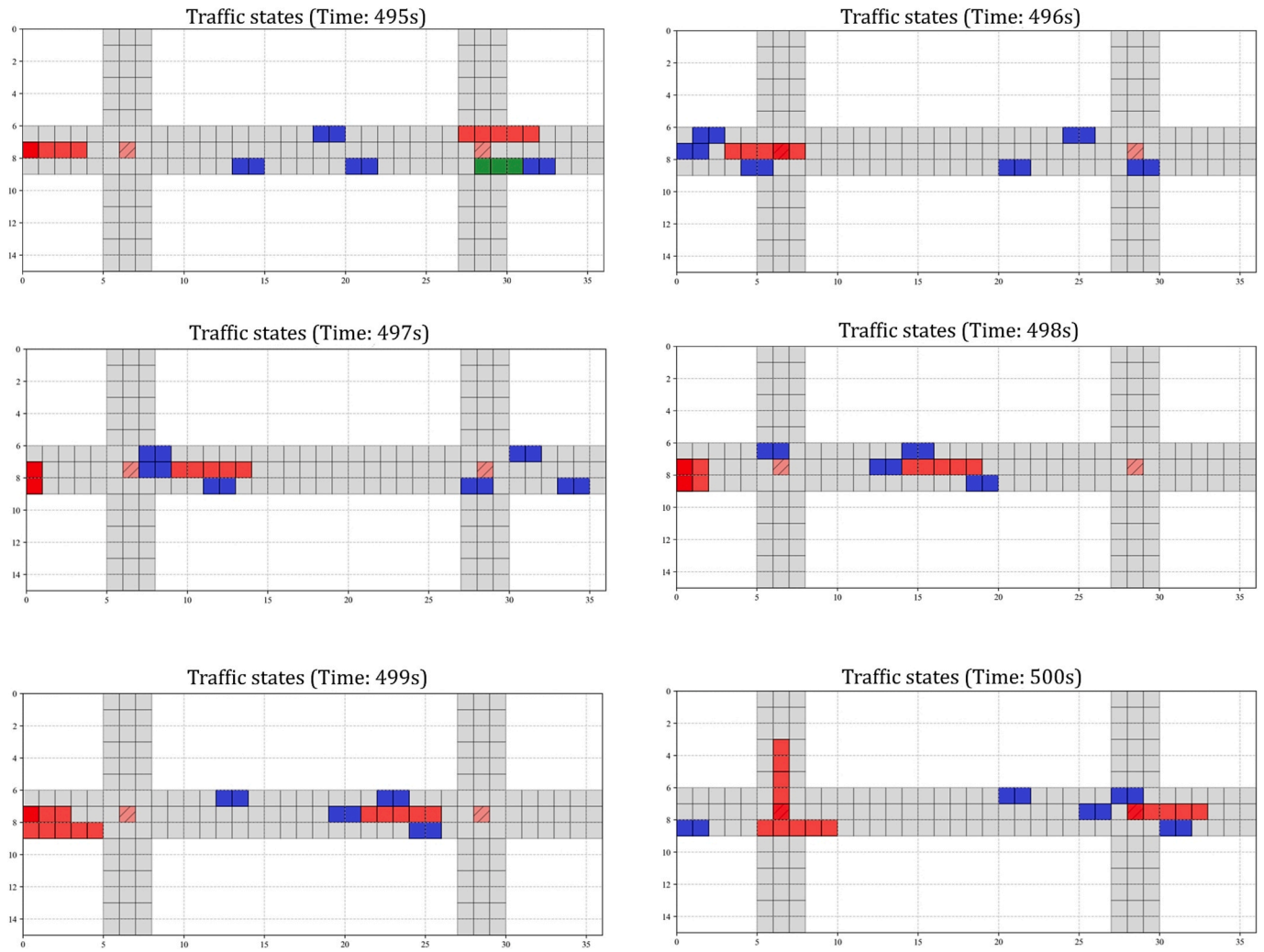


Fig. 12. CA simulated traffic states in Experiment 2 (sec 495–500).

vehicle and the horizontal axis represents the time; the blue solid line represents the current speed of the vehicle, while the red dotted line represents the current following distance. It can be observed that the curve of the following distance always stays within the safe following range, hardly touches the warning zone, and always maintains a high safe distance while maintaining the safe distance. This feature suggests that the predictive support mechanism not only improves the stability of the speed but also provides a safer redundancy in the following behaviour. In addition, the synergistic change in speed and following distance suggests that the vehicle was able to quickly align with the speed of surrounding vehicles after entering the queue:

A more significant improvement is seen in the recovery time metric. The system further calculates the “Speed Recovery Time” indicator, which is the time step required to recover from the lowest point of speed to a stable operating speed. Before the optimisation, the average recovery time for a family car experiencing a speed drop was as high as 48 steps, whereas, with the introduction of the SSA-LSTM control mechanism, this value drops to 1 step. This means the system recognises the downward speed trend in time and quickly guides the vehicle through the buffering process to return to a stable operating state. The improvement in buses is also significant. The average recovery time is reduced from 35 to 19 steps, indicating that heavy vehicles are more responsive under predictive control as data in Table 7 implies:

As shown in Table 8 and Table 9, the frequency of occurrence of each type of vehicle in the optimised group is significantly more even than that of the control group, especially in the occurrence probability of

trucks. Since the experimental setup was set up to impose restrictions on trucks when the road is congested, the increased probability of trucks appearing after the optimisation precisely means that the algorithmic diversion helps greatly in relieving the pressure at the intersection.

The optimised control system effectively reduces the degree of vehicle congregation and improves the longitudinal space utilisation and comfort of the vehicle these results ask presented in Fig. 16.

Since the experimental designs of Experiments 1 and 2 are similar, and Experiment 2 features a higher number of vehicle injections and a more realistic simulation of real-world road conditions, I decided to use Experiment 2 as the representative case, adding a control group to compare the results of the 'basic control group' with those of the 'basic LSTM algorithm optimisation.'

As shown in Fig. 17, (1) and (2) represent speed data for different models before and after optimisation in Experiment 2, while (3) and (4) represent quantity data for different models before and after optimisation in Experiment 2. From the figure, it can be observed that if only the basic LSTM algorithm is introduced for optimisation, the results are almost indistinguishable from those of the basic control group. This is because the LSTM algorithm primarily serves a predictive function. Additionally, without the cooperation of other algorithms, in the experimental design where both upstream and downstream intersections are present, the LSTM algorithm may fail to simultaneously control both upstream and downstream intersections, thereby preventing improvements in traffic congestion.

Therefore, in previous intelligent transportation system research,

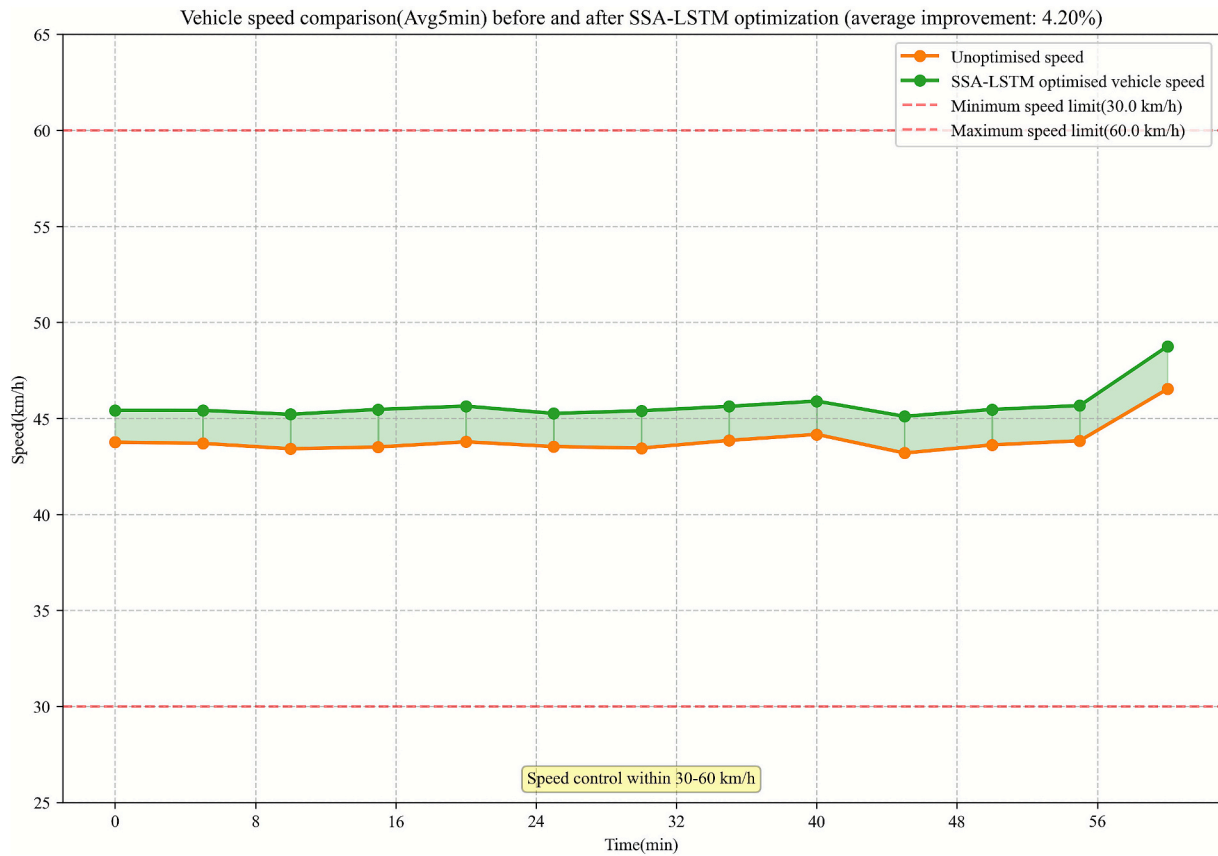


Fig. 13. Comparison of vehicle speed before and after optimisation in Experiment 2.

Table 6  
Speed comparison data in experiment 2.

Time [minutes]	Un-optimised Speed [km/h]	Optimised Speed [km/h]	Improvement [%]
5	43,64	45,41	4,07
10	43,38	45,20	4,21
15	43,43	45,45	4,65
20	43,67	45,60	4,41
25	43,47	45,22	4,02
30	43,38	45,36	4,58
35	43,77	45,49	3,94
40	44,08	45,84	3,99
45	43,11	45,02	4,42
50	43,59	45,41	4,17
55	43,84	45,69	4,23
60	46,42	48,68	4,88

LSTM is typically combined with algorithms such as GNN, CNN, and ant colony algorithms. Depending on the optimisation objectives, it is necessary to use other information processing models in conjunction with the LSTM algorithm to achieve comprehensive control.

The experiments in this section verify the buffering and recovery ability of the predictive support control strategy in traffic fluctuations by constructing high-density injection scenarios and bottleneck perturbations. The optimised group outperforms the control group regarding speed response efficiency, indicating that the LSTM model effectively enhances the system's evacuation capability. As evidenced by the data in the graphs, the predictive control function of LSTM is well-confirmed in high-density scenarios.

### 7.3. Traffic accident experimental environment

Sudden traffic accidents usually lead to the functional degradation of

a specific road section, which triggers queuing and speed fluctuations and may even cause widespread traffic congestion. In intelligent control systems, how to effectively adjust the rhythm of traffic flow after an accident to avoid the propagation of traffic shock waves is an important criterion to test the robustness of control strategies. In this section, a simulated traffic accident obstacle is set up, and the accident vehicle is placed in a fixed area to construct a traffic system operating environment under strong interference conditions and to verify the rhythm coordination and spread suppression ability of the predictive control mechanism based on the SSA-LSTM model under the accident interference.

Based on the three-lane structure, Experiment 3 simulates a vehicular accident scenario in the middle section of the road (an intersection close to a residential area), where a group of static, immovable vehicles is set up to continuously obstruct the typical passage of some lanes. The total number of steps in the simulation was 1000, and the incident was set at step 300 of the simulation, with the incident area set to create an observable traffic disturbance response.

The optimal control group will continue to use the SSA-optimised LSTM model for speed prediction in the next three steps and make speed adjustments in advance in conjunction with the distance and trend decisions; the control group will use the traditional rule-based control mechanism to follow the response based on the current distance difference only.

Fig. 18 shows the change in traffic for the optimised group simulated from the 1127th to the 1232nd second after the accident. It can be observed that the green truck parked in the middle of the road is the vehicle in which the accident occurred. In the simulation demonstration, the blue family sedan, which was initially driving in the middle lane, actively completed the avoidance after approaching the accident vehicle and chose to change lanes and go around, successfully avoiding the danger of rear-end collision through active, intelligent judgment (Wan

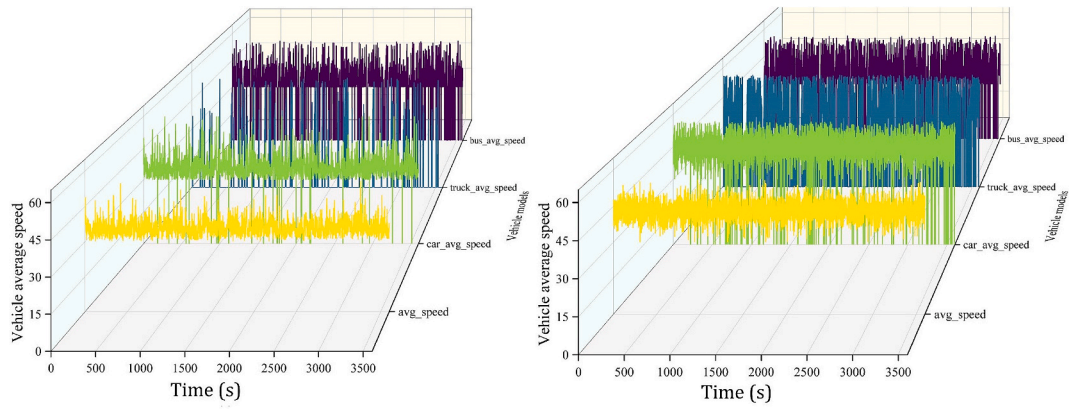


Fig. 14. Speed data for different car models before and after optimisation in Experiment 2.

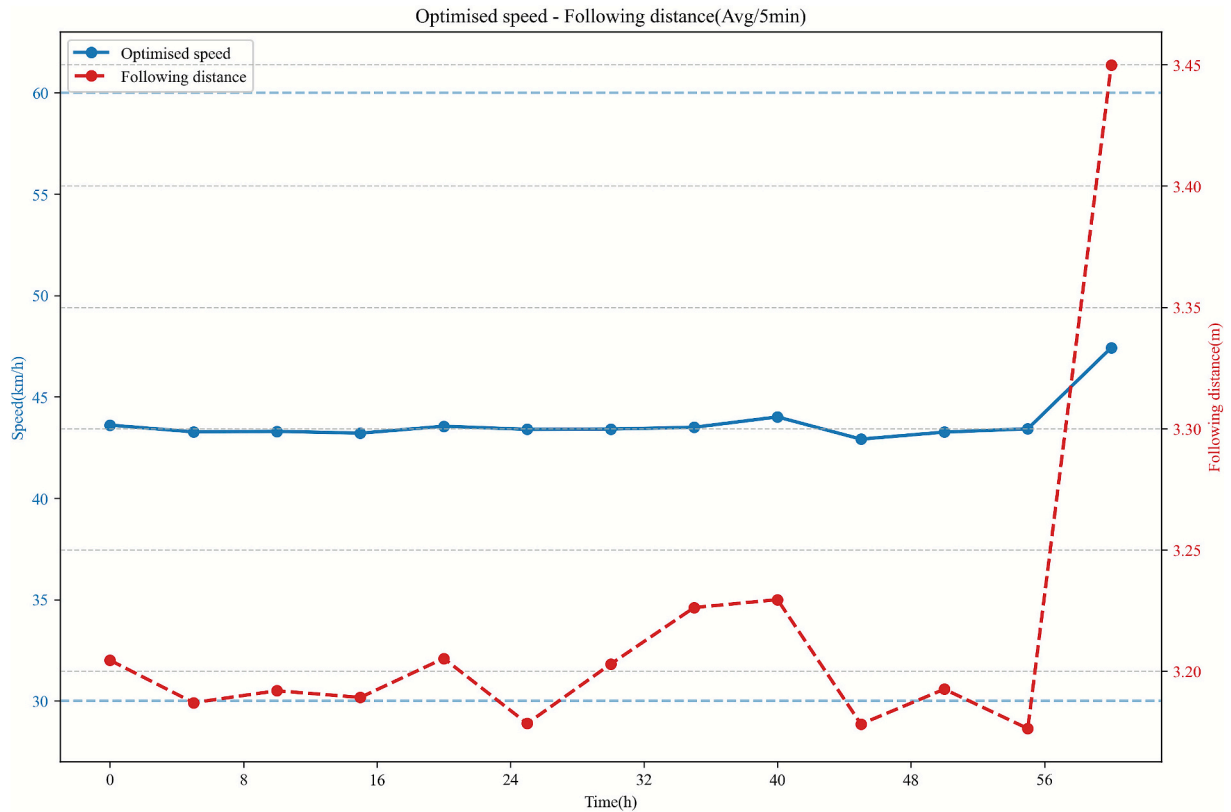


Fig. 15. Vehicle speed versus following distance after optimisation in experiment 2.

**Table 7**  
Comparison of family car and bus speed data in Experiment 2.

Vehicle type	Before Optimisation	After Optimisation
car average speed [km/h]	41,06	46,78
car recovery time [step]	48,00	1,00
bus average speed [km/h]	23,30	27,99
bus recovery time [step]	35,00	19,00

et al., 2024).

As shown in Fig. 19, the image 'Comparison of queuing vehicles before and after SSA-LSTM optimisation' demonstrates the trend of the vehicle queue length during the system operation cycle under the accident scenario, with the horizontal axis being the simulation. The horizontal axis is the simulation time (in minutes), and the vertical axis is the

**Table 8**  
Vehicle access to road proportionality regulation data in experiment 2 (Before Optimisation).

Time Range [s]	Car	Truck	Bus
0-720	79,18 %	0,90 %	19,91 %
720-1440	70,05 %	1,64 %	28,31 %
1440-2160	73,99 %	3,09 %	22,92 %
2160-2880	64,73 %	3,54 %	31,73 %
2880-3600	78,37 %	0,07 %	21,56 %

total number of queuing vehicles counted in the system. The queue change curves for the optimised and un-optimised control groups are plotted using a two-line comparison, where the green line represents the SSA-LSTM control strategy, and the red line represents the system response performance of the traditional rule-based control mechanism

**Table 9**  
Vehicle access to road proportionality regulation data in experiment 2 (After Optimisation).

Time Range [s]	Car	Truck	Bus
0–720	63,86 %	9,37 %	26,58 %
720–1440	53,18 %	27,21 %	19,79 %
1440–2160	67,27 %	12,93 %	20,00 %
2160–2880	50,64 %	19,49 %	30,05 %
2880–3600	58,65 %	7,02 %	34,34 %

in the face of road accident perturbations. The yellow area represents the time from a crash leading to the stationary area where the accidental vehicle resides until the accidental vehicle is removed. At the beginning of the accident, the set point arrives (around minute 20), and the queue length of the un-optimised control group increases rapidly. It maintains

a high level of fluctuation in the middle and late stages of the simulation, with a peak of more than 28 vehicles at one point. The failure of the traditional control strategy to adjust the rhythm before entering the accident area leads to a sharp compression of the distance between vehicles, a multi-point chain braking phenomenon. In contrast, the queuing curve of the optimisation group rises at a much slower slope, and the maximum value is significantly limited, with at most six vehicles in congestion, which is 78.6 % less than that of the control group, and falls back quickly after stabilising the situation through algorithmic interference:

According to the graph, the average queue length for the un-optimised control group was 19.6 vehicles in the ten minutes after the accident, with a peak of 28 vehicles at one point, while the average queue length for the optimised group was stable at 1.4 vehicles, with a peak of up to 6 vehicles. This shows that the SSA-LSTM algorithm can effectively respond to accidental events in the traffic environment, this

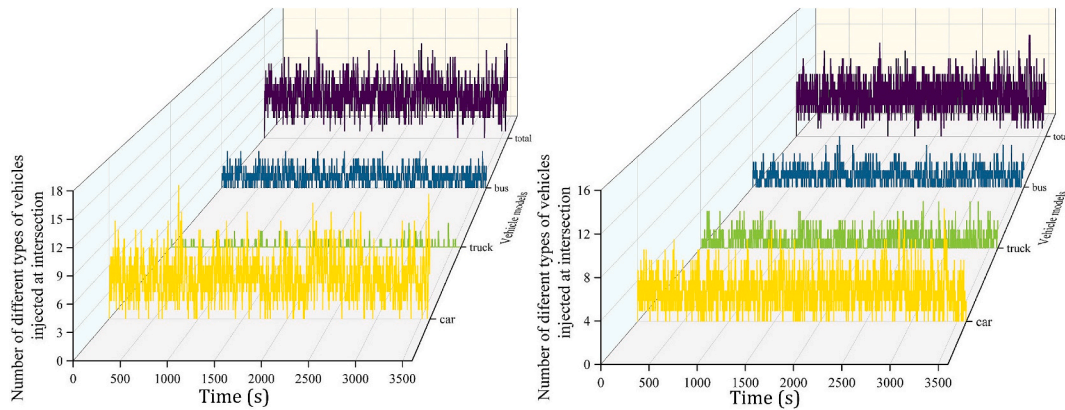


**Fig. 16.** Quantity data for different models before and after optimisation in Experiment 2.

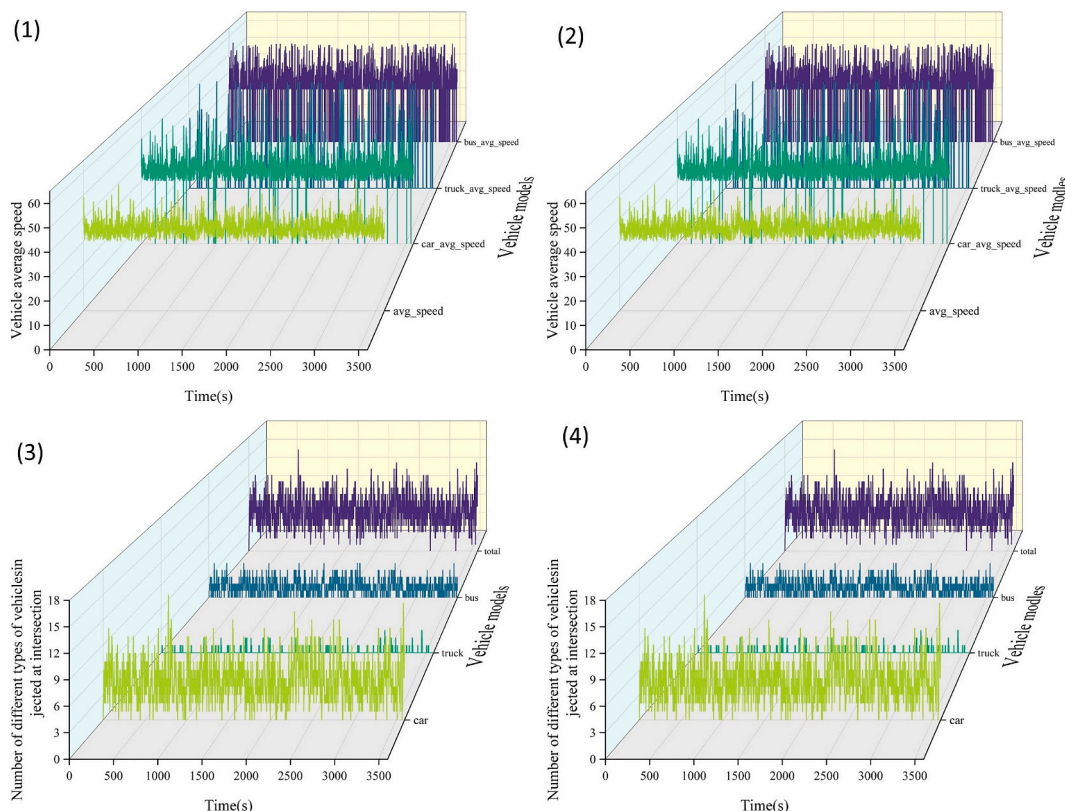


**Fig. 17.** Speed and quantity data for different models before and after basic LSTM optimisation in Experiment 2.

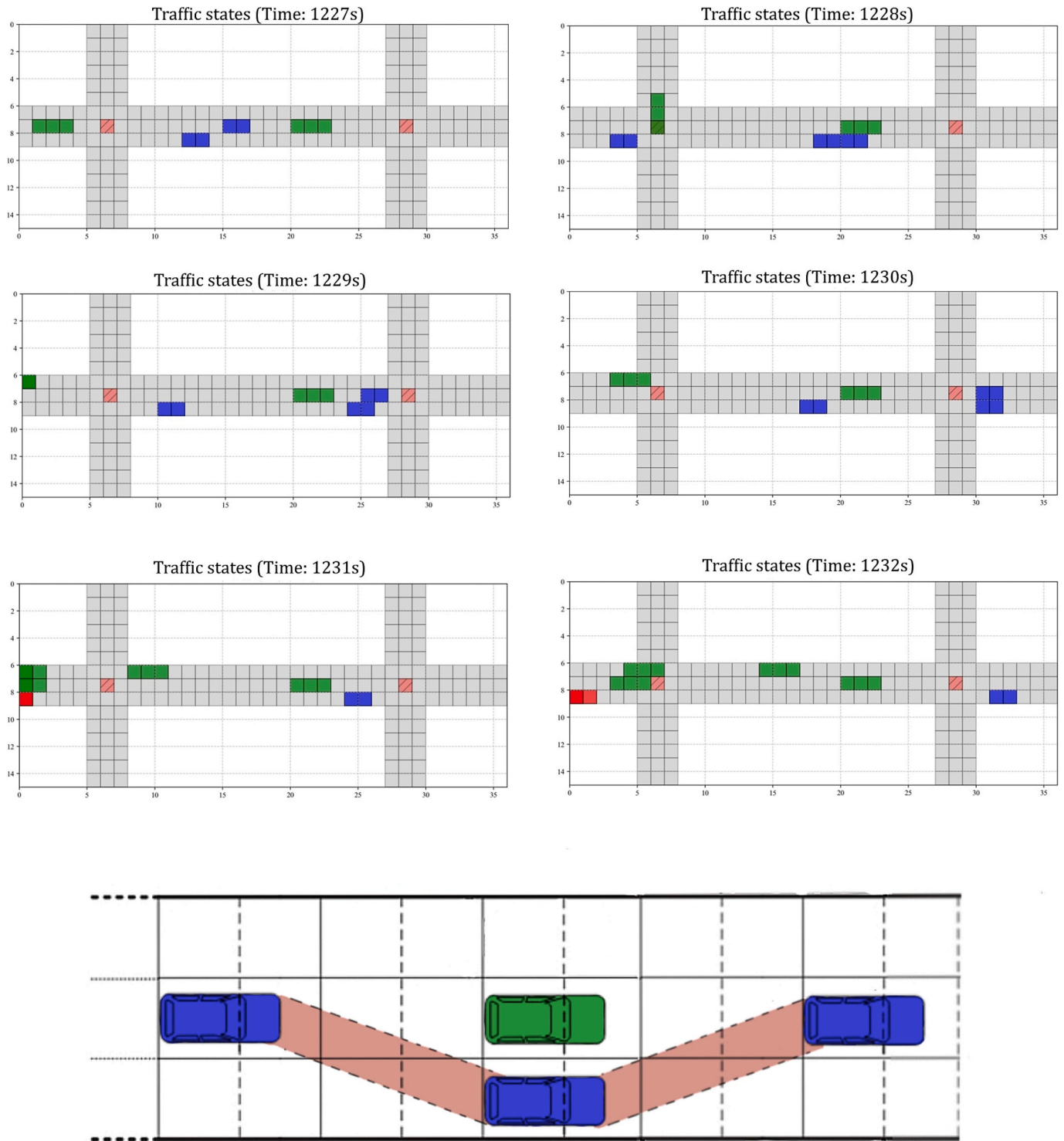


Fig. 18. CA simulated traffic states in Experiment 3 (sec 1227–1232).

data and improvement percentage is summarized in Table 10. Regulating vehicle lane changing and steering can ensure the responsiveness and safety of autonomous vehicles.

Experiment 3 verifies the ability of the SSA-LSTM control strategy to regulate the vehicle in response to unexpected accidents. The algorithm is high-speed and effective in controlling the range of the queuing area without letting the vehicles queue up to an uncontrollable degree. It does not cause congestion on the road. The comprehensive analysis results show that the predictive control mechanism is highly adaptive to

non-regular changes under multiple overlapping disturbance scenarios and provides scalable model support for urban multi-situation deployment.

## 8. Conclusion and discussion on future research

This study proposes an integrated methodological framework combining deep learning prediction and adaptive control strategies for speed prediction and longitudinal control in intelligent transport

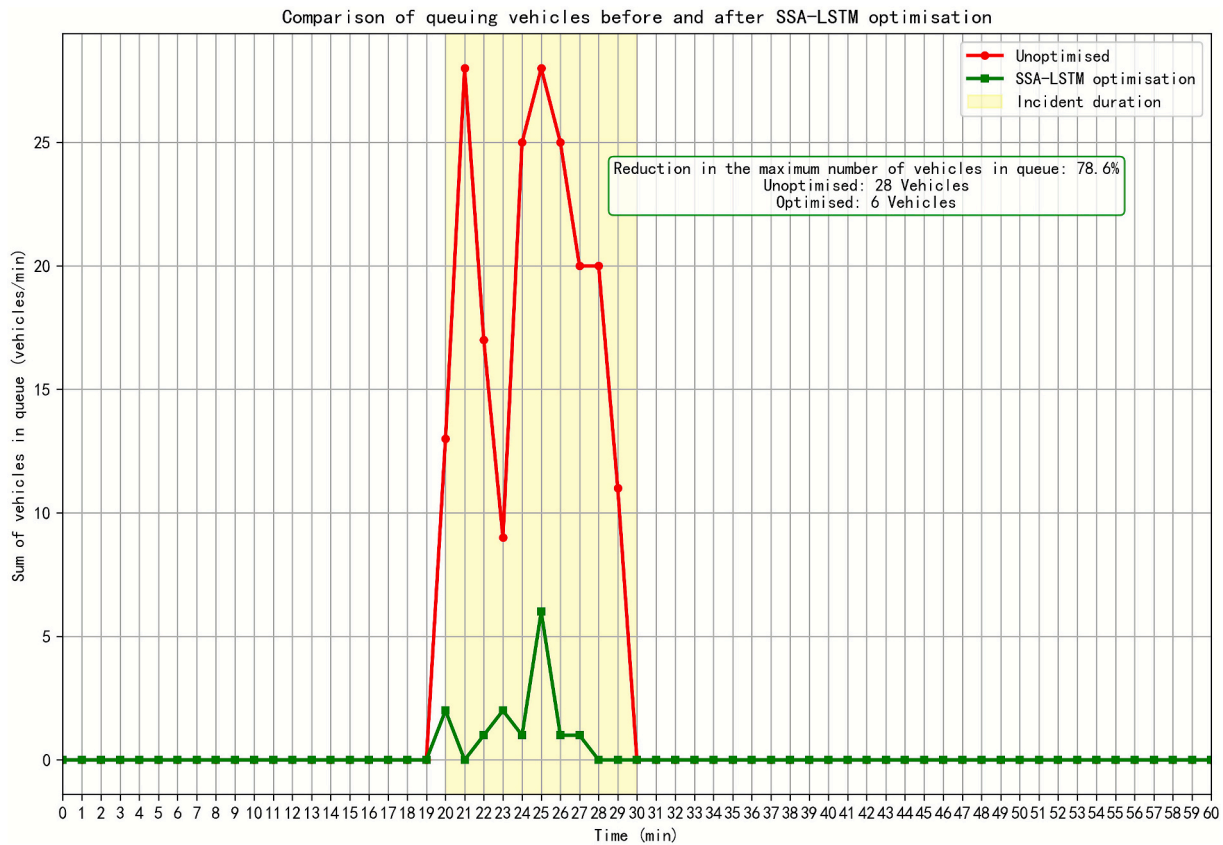


Fig. 19. Comparison of queuing vehicles before and after SSA-LSTM optimisation in experiment 3.

Table 10  
Queuing length comparison.

During the accident	Before Optimisation	After Optimisation	Improvement [%]
Average Queue [Vehicles]	19,60	1,40	92,86
Max Queue [Vehicles]	28,00	6,00	78,57

systems and verified by multiple sets of experiments on a self-developed microscopic traffic simulation platform.

This study addresses autonomous driving vehicles, improves the efficiency of vehicle systems' automatic judgement and response, and effectively reduces the response processing time when the vehicle encounters various accidental conditions on the road. In the traffic flow, all vehicles' travelling speeds and safe travelling distances are guaranteed, which has been demonstrated in both theoretical and experimental results.

Therefore, this study has achieved comprehensive coverage in multiple aspects of the theoretical and systematic experimental design for traffic research of autonomous vehicles. Combining ACC and SSA-LSTM algorithms has realised the overall research objectives.

As autonomous driving technology evolves from the perception layer to the decision and control layer, vehicle intelligence no longer relies solely on passive responses but shifts to active control mechanisms with prediction and regulation capabilities. The system architecture proposed in this study, which is based on the deep fusion of the LSTM speed prediction model optimised by the sparrow search algorithm and adaptive cruise control (ACC), is just right to satisfy the core needs of the autonomous driving control system in terms of behavioural foresight, rhythmic stability and microscopic synergy. The control framework can be embedded into the intelligent control chain of the autonomous

vehicle as the prediction module of the ACC controller to enhance the vehicle's dynamic response capability in complex road conditions such as high-density traffic, ramp convergence, and urban signal zones. The prediction mechanism identifies future speed trends by analysing historical data to achieve front identification and speed regulation of vehicle distance changes, thus slowing down the braking chain effect, reducing fuel consumption and safety risks, and improving the comfort of following the vehicle. In urban roads, the model can be combined with traffic light information to achieve green wave speed regulation; in high-speed scenarios, lane change and queue fusion control can be accomplished through roadside units or on-board modules in collaboration; in scenarios affected by unexpected accidents, the prediction mechanism can also support pre-accident vehicles to achieve adaptive tempo mitigation to avoid forced braking and queue compression. At the same time, the modular meta cellular automata simulation platform constructed in this study can also interface with the digital twin platform, which provides a good foundation for the iterative validation and virtual deployment of autonomous driving strategies.

As the traffic flow simulations in the three experiments of this study were based on programme-set parameter inputs rather than real traffic flow datasets, discrepancies may arise between actual traffic diversion outcomes and experimental simulations when applied to real-world conditions. The data calculated in this experiment represent idealised scenarios, and numerous real-world road condition errors that could influence experimental simulations were not fully accounted for in this research. For instance, real-world scenarios may involve a greater variety of vehicle types and necessitate observation of more vehicle sizes, which could influence road congestion levels. Furthermore, given that the simulated road conditions are situated near residential areas, pedestrians may be present on the roads. This poses a challenge to the fleet's responsiveness, where even minor miscalculations could lead to accidents. Moreover, real-world scenarios involve more complex

interactions between upstream and downstream vehicles. Achieving precise overall vehicle scheduling presents a significant challenge for this research. Consequently, the feasibility of the experimental results in practical applications requires further investigation and validation. Integrating the control scheme developed in this study with real traffic data for subsequent experiments is part of the researchers' plans.

Future research can be expanded and deepened in several ways. First and foremost, more complex sequence modelling networks at the predictive model level, such as the Transformer architecture based on the attention mechanism, should be introduced to enhance the modelling capability of long-distance state correlations. On the other hand, a reinforcement learning mechanism is introduced into the controller architecture to equip the control logic with self-learning and self-tuning parameterisation capabilities over multiple simulation trials to enhance further the system's adaptive level in response to unknown disturbances. In addition, the control objectives in this study will observe each other, i.e., make each autonomous vehicle in the traffic flow a part of the whole and, at the same time, cluster into a controllable whole that will influence each other. The simulation system used in this study allows for prediction and control by reading traffic data. With the help of judgemental commands and vehicle sensing data, it is expected that the feasibility of the control system can be further verified in the future, even in a real road environment.

#### Ethics statement

Not applicable. This study does not involve human participants, animals, or data from social media.

#### Declaration of generative AI and AI-assisted technologies in the writing process

The authors affirm that all language and content in this publication were generated without the use of AI techniques.

#### Funding statement

This research was supported by the Hungarian Research Fund (OTKA K143595).

#### CRedit authorship contribution statement

**Tao Yufei:** Writing – original draft, Visualization, Validation, Software, Methodology, Conceptualization. **Husam A. Neamah:** Writing – review & editing, Writing – original draft, Validation, Supervision, Methodology, Conceptualization.

#### Declaration of competing interest

The authors declare that they have no known competing financial interests or personal relationships that could have appeared to influence the work reported in this paper.

#### Acknowledgments

The authors would like to thank the University of Debrecen for support through its Program for Scientific Publication. also we appreciate the support by the Hungarian Research Fund (OTKA K143595).

#### Data availability

No data was used for the research described in the article.

#### References

- Abdel-Aty, M., Ding, S., 2024. A matched case-control analysis of autonomous vs human-driven vehicle accidents. *Nat. Commun.* 15 (1), 4931. <https://doi.org/10.1038/s41467-024-48526-4>.
- Abdessalem, R.B., Nejati, S., Briand, L.C., Stifter, T., 2018. Testing vision-based control systems using learnable evolutionary algorithms. *Proceedings of the 40th International Conference on Software Engineering*, 1016–1026. <https://doi.org/10.1145/3180155.3180160>.
- Abdessalem, R.B., Panichella, A., Nejati, S., Briand, L.C., Stifter, T., 2018b. Testing autonomous cars for feature interaction failures using many-objective search. In: *Proceedings of the 33rd ACM/IEEE International Conference on Automated Software Engineering*, pp. 143–154. <https://doi.org/10.1145/3238147.3238192>.
- Almusawi, H., Al-Jabali, M., Khaled, A., Korondi, P., Husi, G., 2022. Self-Driving robotic car utilizing image processing and machine learning. *IOP Conf. Ser.: Mater. Sci. Eng.* 1256, 012024. <https://doi.org/10.1088/1757-899X/1256/1/012024>.
- Amir Siddique, M., Wang, Y., Xu, N., Ullah, N., Zeng, P., 2021. The spatiotemporal implications of urbanization for urban heat islands in Beijing: a predictive approach based on CA-Markov Modeling (2004–2050). *Remote Sens. (Basel)* 13 (22), 4697. <https://doi.org/10.3390/rs13224697>.
- Ban, Y., Zhang, Y., Tong, H., Banerjee, A., He, J., 2022. Improved algorithms for neural active learning. *Adv. Neural Inf. Process. Syst.* 35, 27497–27509.
- Baqa, M.F., Chen, F., Lu, L., Qureshi, S., Tariq, A., Wang, S., Jing, L., Hamza, S., Li, Q., 2021. Monitoring and modeling the patterns and trends of urban growth using urban sprawl matrix and CA-Markov model: a case study of Karachi Pakistan. *Land* 10 (7), 700. <https://doi.org/10.3390/land10070700>.
- Ben Abdessalem, R., Nejati, S., Briand, L.C., Stifter, T., 2016. Testing advanced driver assistance systems using multi-objective search and neural networks. In: *Proceedings of the 31st IEEE/ACM International Conference on Automated Software Engineering*, pp. 63–74. <https://doi.org/10.1145/2970276.2970311>.
- Bharti, R.P., Kumar, K., 2023. Short-term traffic flow prediction based on optimized deep learning neural network: PSO-Bi-LSTM. *Physica A* 625, 129001. <https://doi.org/10.1016/j.physa.2023.129001>.
- Bonivento, C., Dondi, G., Paoli, A., Sartini, M., Simone, A., 2011. Modular model building for vehicular traffic systems with macroscopic dynamics\*. *IFAC Proceedings Volumes* 44 (1), 13876–13881. <https://doi.org/10.3182/20110828-6-IT-1002.02133>.
- Bryant, D., Huson, D.H., 2023. NeighborNet: improved algorithms and implementation. *Front. Bioinform.* 3, 1178600. <https://doi.org/10.3389/fbinf.2023.1178600>.
- Cabrejas-Egea, A., Zhang, R., Walton, N., 2021. Reinforcement learning for traffic signal control: comparison with commercial systems. *Transp. Res. Procedia* 58, 638–645. <https://doi.org/10.1016/j.trpro.2021.11.084>.
- Cardoso, R., Kokkinogenis, Z., Rossetti, J.F., Emilio Almeida, J., 2023. Traffic light management for automated guided vehicle systems using deep reinforcement learning. *Proceedings of the 35th European Modeling & Simulation Symposium, EMSS. the 35th European Modeling & Simulation Symposium*.
- Chen, J., Tang, C., Xin, L., Li, S.E., Tomizuka, M., 2018. Continuous decision making for on-road autonomous driving under uncertain and interactive environments. *IEEE Intelligent Vehicles Symposium (IV) 2018*, 1651–1658. <https://doi.org/10.1109/IVS.2018.8500605>.
- Chen, Y., 2024. Motion planning for autonomous driving: Navigating through traffic interactions under constraints (p. 991013340444803412) [Ph.D., The Hong Kong University of Science and Technology]. <https://doi.org/10.14711/thesis-991013340444803412>.
- Czarniecki, K., 2018a. Automated driving system (ADS) task analysis part 2: structured road maneuvers. *Waterloo Intelligent Systems Engineering Lab (WISE) Report*.
- Czarniecki, K., 2018. Operational World Model Ontology for Automated Driving Systems. *Waterloo Intelligent Systems Engineering Lab (WISE) Report*.
- Di Lillo, L., Gode, T., Zhou, X., Atzei, M., Chen, R., Victor, T., 2024. Comparative safety performance of autonomous- and human drivers: a real-world case study of the Waymo driver. *Heliyon* 10 (14), e34379. <https://doi.org/10.1016/j.heliyon.2024.e34379>.
- Elrofai, H., Worm, D., Op den Camp, O., 2016. Scenario identification for validation of automated driving functions. In: Schulze, T., Müller, B., Meyer, G. (Eds.), *Advanced Microsystems for Automotive Applications 2016*. Springer International Publishing, pp. 153–163. [https://doi.org/10.1007/978-3-319-44766-7\\_13](https://doi.org/10.1007/978-3-319-44766-7_13).
- Eskandarian, A., 2024. Advanced methods and algorithms for selected connected autonomous vehicles (CAVs) benefits. *IEEE Trans. Intell. Transp. Syst.* 25 (4), 405–442. <https://doi.org/10.1109/TITS.2024.3376268>.
- Francis, L., Guda, B., Biyabani, A., 2024. Optimizing traffic signal control using high-dimensional state representation and efficient deep reinforcement learning. *arXiv: 2411.07759*.
- Gao, F., Luo, C., Shi, F., Chen, X., Gao, Z., Zhao, R., 2023. Online safety verification of autonomous driving decision-making based on dynamic reachability analysis. *IEEE Access* 11, 93293–93309. <https://doi.org/10.1109/ACCESS.2023.3300423>.
- de Gelder, E., Paardekooper, J.-P., Saberi, A.K., Elrofai, H., den Camp, O.O., Kraines, S., Ploeg, J., Schutter, B.D., 2022. Towards an ontology for scenario definition for the assessment of automated vehicles: an object-oriented framework. *IEEE Trans. Intell. Veh.* 7 (2), 300–314. <https://doi.org/10.1109/ITV.2022.3144803>.
- Ghods, Z., Hari, S.K.S., Frosio, I., Tsai, T., Troccoli, A., Keckler, S.W., Garg, S., Anandkumar, A., 2021. Generating and characterizing scenarios for safety testing of autonomous vehicles (No. arXiv:2103.07403). *arXiv: https://doi.org/10.48550/arXiv.2103.07403*.
- Han, Y., Guo, L., Chen, H., 2024. Value conditional state entropy reinforcement learning for autonomous driving decision making. In: *2024 IEEE 22nd International*

- Conference on Industrial Informatics (INDIN), pp. 1–6. <https://doi.org/10.1109/INDIN58382.2024.10774316>.
- Harrou, F., Zeroual, A., Kadri, F., Sun, Y., 2024. Enhancing road traffic flow prediction with improved deep learning using wavelet transforms. *Results Eng.* 23, 102342. <https://doi.org/10.1016/j.rineng.2024.102342>.
- He, X., Lv, C., 2023. Towards safe autonomous driving: decision making with observation-robust reinforcement learning. *Automot. Innov.* 6 (4), 509–520. <https://doi.org/10.1007/s42154-023-00256-x>.
- Hu, Y., Rey, D., Mohajerpoor, R., Saberi, M., 2024. Optimizing traffic signal control for continuous-flow intersections: benchmarking against a state-of-practice model. *IET Intel. Transport Syst.* 18 (11), 2152–2165. <https://doi.org/10.1049/itr2.12559>.
- Huang, C., Lv, C., 2021. Towards safe and personalized autonomous driving: decision-making and motion control with DPF and CDT techniques. *IEEE/ASME Trans. Mechatron.* 26 (2), 611–620. <https://doi.org/10.1109/TMECH.2021.3053248>.
- Jiang, Y., Wang, S., Yao, Z., Zhao, B., Wang, Y., 2021. A cellular automata model for mixed traffic flow considering the driving behavior of connected automated vehicle platoons. *Physica A* 582, 126262. <https://doi.org/10.1016/j.physa.2021.126262>.
- Jin, M., Qu, M., Gao, Q., Huang, Z., Su, T., Liang, Z., 2024. Advanced trajectory planning and control for autonomous vehicles with quintic polynomials. *Sensors* 24 (24), 7928. <https://doi.org/10.3390/s24247928>.
- Kang, D., Lv, Y., Chen, Y., 2017. Short-term traffic flow prediction with LSTM recurrent neural network. In: 2017 IEEE 20th International Conference on Intelligent Transportation Systems (ITSC), pp. 1–6. <https://doi.org/10.1109/ITSC.2017.8317872>.
- Katona, K., Neamah, H.A., Korondi, P., 2024. Obstacle avoidance and path planning methods for autonomous navigation of mobile robot. *Sensors* 24 (11), 11. <https://doi.org/10.3390/s24113573>.
- Katz-Samuels, J., Zhang, J., Jain, L., Jamieson, K., 2021. Improved algorithms for agnostic pool-based active classification. *International Conference on Machine Learning*.
- Kövári, B., Szőke, L., Bécsi, T., Aradi, S., Gáspár, P., 2021. Traffic signal control via reinforcement learning for reducing global vehicle emission. *Sustainability* 13 (20), 11254. <https://doi.org/10.3390/su132011254>.
- Lí, C., Liu, S., Cen, X., 2021. Safety and efficiency impact of pedestrian–vehicle conflicts at non signalized midblock crosswalks based on fuzzy cellular automata. *Physica A* 572, 125871. <https://doi.org/10.1016/j.physa.2021.125871>.
- Lí, H., Zhao, Y., Ma, C., Wang, K., Huang, X., Zhang, W., 2022. Short-term passenger flow prediction of urban rail transit based on SDS-SSA-LSTM. *J. Adv. Transp.* 2022, 1–11. <https://doi.org/10.1155/2022/2589681>.
- Lí, Y., Luo, D., Wang, J., Ding, W., Song, Y., 2025. Mitigating cascading effects of vehicle lane changes: a hyperedge game approach. *Transp. Res. Part C Emerging Technol.* 171, 104971. <https://doi.org/10.1016/j.trc.2024.104971>.
- Liu, W., 2024. Situation-aware autonomous driving decision making with cooperative perception on demand (No. arXiv:2409.01504). arXiv. <https://doi.org/10.48550/arXiv.2409.01504>.
- Luo, Y., Zhang, X.-Y., Arcaini, P., Jin, Z., Zhao, H., Ishikawa, F., Wu, R., Xie, T., 2021. Targeting requirements violations of autonomous driving systems by dynamic evolutionary search. In: 2021 36th IEEE/ACM International Conference on Automated Software Engineering (ASE), pp. 279–291. <https://doi.org/10.1109/ASE51524.2021.9678883>.
- Masuk, A., Orosz, M.K.A., Neamah, H.A., Balajti, I., 2022. Cyber-physical system aspects of microstrip patch antenna of radar sensor application. 23rd Proceedings International Radar Symposium, 418–423. DEENK-PA.
- Montanaro, U., Dixit, S., Fallah, S., Dianati, M., Stevens, A., Oxtoby, D., Mouzakitis, A., 2019. Towards connected autonomous driving: review of use-cases. *Veh. Syst. Dyn.* 57 (6), 779–814. <https://doi.org/10.1080/00423114.2018.1492142>.
- Moreno-Malo, J., Posadas-Yagüe, J.-L., Cano, J.C., Calafate, C.T., Conejero, J.A., Pozalujan, J.-L., 2024. Improving traffic light systems using deep Q-networks. *Expert Syst. Appl.* 252, 124178. <https://doi.org/10.1016/j.eswa.2024.124178>.
- Nath, B., Wang, Z., Ge, Y., Islam, K., Singh, P., 2020. Land use and land cover change modeling and future potential landscape risk assessment using Markov-CA model and analytical hierarchy process. *ISPRS Int. J. Geo Inf.* 9 (2), 134. <https://doi.org/10.3390/ijgi9020134>.
- Neamah, H.A., Alghazawi, M., Korondi, P., 2024a. Multi-agents trajectory prediction for autonomous vehicles with multi-modal predictions. In: 2024 IEEE 15th International Conference on Cognitive Infocommunications (CogInfoCom), pp. 000259–000264. <https://doi.org/10.1109/CogInfoCom63007.2024.10894711>.
- Neamah, H.A., Butdee, R., 2024a. B-splined trajectory modified generation to maximize speed of the nonholonomic AMR robot. *J. Mach. Eng.* 24. <http://jmacheng.net/pl/pdf-196037-116709?filename=116709.pdf>.
- Neamah, H.A., Butdee, R., 2024. Optimization modeling parameters for industrial AMR slippage using ANFIS system in dynamic environment. In P. Janmanee, S. Chujarjeen, S. Butdee, P. Srihumsuk, A. D. L. Batako, A. Burduk, & M. A. Xavier (Eds), *Advanced in Creative Technology- added Value Innovations in Engineering, Materials and Manufacturing* (Vol. 979, pp. 214–223). Springer Nature Switzerland. [https://doi.org/10.1007/978-3-031-59164-8\\_18](https://doi.org/10.1007/978-3-031-59164-8_18).
- Neamah, H.A., Donát, E.A., Korondi, P., 2024b. Optimizing autonomous navigation in unknown environments: a novel trap avoiding vector field histogram algorithm VFH +T. *Res. Eng.* 1–29, DEENK-PA. <https://doi.org/10.1016/j.rineng.2024.102625> in Press.
- Neamah, H.A., Dulaimi, M., Silavinia, A., Babangida, A.A., Szemes, P.T., 2024c. Development of a Volkswagen Jetta MK5 hybrid vehicle for optimized system efficiency based on a genetic algorithm. *Energies* 17 (5), 1–25. <https://doi.org/10.3390/en17051116>. DEENK-PA.
- Neamah, H.A., Mayorga Mayorga, O.A., 2024. Optimized TD3 algorithm for robust autonomous navigation in crowded and dynamic human-interaction environments. *Results Eng.* 24, 102874. <https://doi.org/10.1016/j.rineng.2024.102874>.
- Nilsson, J., Brännström, M., Coelingh, E., Fredriksson, J., 2017. Lane change maneuvers for automated vehicles. *IEEE Trans. Intell. Transp. Syst.* 18 (5), 1087–1096. <https://doi.org/10.1109/ITITS.2016.2597966>.
- Nyangaresi, V.O., Abduljabbar, Z.A., Mutlag, K.-A.-A., Bulbul, S.S., Ma, J., Aldarwish, A. J.Y., Alshuwaili, D.G.H., Al, S., Mustafa, A., 2024. Smart city energy efficient data privacy preservation protocol based on biometrics and fuzzy commitment scheme. *Sci. Rep.* 14 (1), 1–17. <https://doi.org/10.1038/s41598-024-67064-z>. DEENK-PA.
- Ranpura, P., Gujar, R., Singh, S., 2025. Development of mixed traffic microsimulation model calibration for signalized intersections. *Transp. Res. Procedia* 82, 2898–2910. <https://doi.org/10.1016/j.trpro.2024.12.226>.
- Rong, G., Shin, B.H., Tabatabaee, H., Lu, Q., Lemke, S., Možeiko, M., Boise, E., Uhm, G., Gerow, M., Mehta, S., Agafonov, E., Kim, T. H., Sterner, E., Ushiroda, K., Reyes, M., Zelenkovsky, D., Kim, S., 2020. LGSVL simulator: a high fidelity simulator for autonomous driving (No. arXiv:2005.03778). arXiv. <https://doi.org/10.48550/arXiv.2005.03778>.
- Sarrab, M., Pulparambil, S., Awadalla, M., 2020. Development of an IoT based real-time traffic monitoring system for city governance. *Global Transitions* 2, 230–245. <https://doi.org/10.1016/j.glt.2020.09.004>.
- Schütt, B., Ransiek, J., Braun, T., Sax, E., 2023. 1001 ways of scenario generation for testing of self-driving cars: a survey (No. arXiv:2304.10850). arXiv. <https://doi.org/10.48550/arXiv.2304.10850>.
- Shafaei, S., Kugele, S., Osman, M.H., Knoll, A., 2018. Uncertainty in machine learning: a safety perspective on autonomous driving. In B. Gallina, A. Skavhaug, E. Schoitsch, & F. Bitsch (Eds), *Computer Safety, Reliability, and Security* (Vol. 11094, pp. 458–464). Springer International Publishing. [https://doi.org/10.1007/978-3-319-99229-7\\_39](https://doi.org/10.1007/978-3-319-99229-7_39).
- Su, T., Zhang, C.-Y., 2024. Multimodal reinforcement learning with dynamic graph representations for autonomous driving decision-making. In: 2024 14th International Conference on Information Science and Technology (ICIST), pp. 866–874. <https://doi.org/10.1109/ICIST63249.2024.10805327>.
- Tan, C., Wang, T., Zhang, M., Yue, T., 2025. Safety behavior abstraction and model evolution in autonomous driving. *Softw. Syst. Model.* <https://doi.org/10.1007/s10270-024-01261-2>.
- Thorn, E., Kimmel, S., Chaka, M., 2018. A framework for automated driving system testable cases and scenarios. National Highway Traffic Safety Administration, Washington, DC.
- Tsuchimochi, T., Ryo, Y., Ten-no, S.L., 2023. Improved algorithms of quantum imaginary time evolution for ground and excited states of molecular systems. *J. Chem. Theory Comput.* 19 (2), 503–513. <https://doi.org/10.1021/acs.jctc.2c00906>.
- Wan, J., Liu, H., Xu, M., Yang, X., Guo, Y., Wang, X., 2024. Lane-changing tracking control of automated vehicle platoon based on MA-DDPG and adaptive MPC. *IEEE Access* PP (99), 1. <https://doi.org/10.1109/ACCESS.2024.3381629>.
- Wang, H., Xu, S., Deng, L., 2021. Automatic lane-changing decision based on single-step dynamic game with incomplete information and collision-free path planning. *Actuators* 10 (8), 173. <https://doi.org/10.3390/act10080173>.
- Wang, Y., Li, J., 2020. Improved algorithms for convex-concave minimax optimization. *Adv. Neural Inf. Process. Syst.* 33, 4800–4810.
- Xu, G., Yang, Z., Xie, S., Bai, S., Liu, Z., 2025. Enhancing safety and efficiency of signal intersections: a part-time protected right-turn signal control for straight-right lane in connected environment. *Physica A* 661, 130378. <https://doi.org/10.1016/j.physa.2025.130378>.
- Xu, M., Liu, H., Yang, H., 2024a. Ensemble learning based approach for traffic incident detection and multi-category classification. *Eng. Appl. Artif. Intel.* 132, 107933. <https://doi.org/10.1016/j.engappai.2024.107933>.
- Xu, X., Shi, X., Chen, Y., Wu, X., 2024b. An ontology-based vehicle behavior prediction method incorporating vehicle light signal detection. *Sensors* 24 (19), 6459. <https://doi.org/10.3390/s24196459>.
- Xue, J., Shen, B., 2020. A novel swarm intelligence optimization approach: sparrow search algorithm. *Syst. Sci. Control Eng.* 8 (1), 22–34. <https://doi.org/10.1080/21642583.2019.1708830>.
- Xue, Q., Xing, Y., Lu, J., 2022. An integrated lane change prediction model incorporating traffic context based on trajectory data. *Transp. Res. Part C Emerging Technol.* 141, 103738. <https://doi.org/10.1016/j.trc.2022.103738>.
- Yan, Y., Liu, C., Chang, F., Huang, Y., 2024. An improved proximal policy optimization algorithm for autonomous driving decision-making. Fourth International Conference on Sensors and Information Technology (ICSI 2024), 13107, 837–845. <https://doi.org/10.1117/12.3029265>.
- Yang, X., Liu, H., Xu, M., Wan, J., 2024. Cooperative merging control based on reinforcement learning with dynamic waypoint. *IEEE Access* PP (99), 1. <https://doi.org/10.1109/ACCESS.2024.3408223>.
- Zhang, J., Gao, Q., Tian, J., Cui, F., Wang, T., 2024. Car-following model based on spatial expectation effect in connected vehicle environment: Modeling, stability analysis and identification. *Physica A* 641, 129747. <https://doi.org/10.1016/j.physa.2024.129747>.
- Zhang, M., Selic, B., Ali, S., Yue, T., Okariz, O., Norgren, R., 2016. Understanding uncertainty in cyber-physical systems: a conceptual model. In A. Wasowski & H.

- Lönn (Eds), Modelling Foundations and Applications (Vol. 9764, pp. 247–264). Springer International Publishing. [https://doi.org/10.1007/978-3-319-42061-5\\_16](https://doi.org/10.1007/978-3-319-42061-5_16).
- Zhang, M., Zhang, Y., Zhang, L., Liu, C., Khurshid, S., 2018. DeepRoad: GAN-based metamorphic testing and input validation framework for autonomous driving systems. In: Proceedings of the 33rd ACM/IEEE International Conference on Automated Software Engineering, pp. 132–142. <https://doi.org/10.1145/3238147.3238187>.
- Zhang, Y., Chen, L., Li, N., 2025. Improved quintic polynomial autonomous vehicle lane-change trajectory planning based on hybrid algorithm optimization. World Electr. Veh. J. 16 (5), 244. <https://doi.org/10.3390/wevj16050244>.